Electromagnetic imaging of a prior stream channel using a DUALEM-421 and inversion

(Yasserie, 2009)

The Rainbow Serpent:
"*…his tracks made the creeks and rivers as he journeyed North*"
(Peckham, 2000)

Kira Bruzgulis

Supervisor:
Dr John Triantafilis

Submitted in partial fulfillment of the requirements for the degree of Bachelor of Science (Advanced Science),
School of Biological, Earth and Environmental Sciences,
Faculty of Science,
The University of New South Wales

November 2009

THE UNIVERSITY OF
NEW SOUTH WALES

Faculty of Science
School of Biological, Earth and Environmental Sciences

Honours Thesis Declaration

I hereby declare that this submission is my own work and to the best of my knowledge it contains no materials previously published or written by another person, nor material which to a substantial extent has been accepted for the award of any other degree or diploma at UNSW or any other educational institution, except where the acknowledgement is made in the thesis. Any contribution made to the research by others, with whom I have worked at UNSW or elsewhere, is explicitly acknowledged in the thesis.

I also declare that the intellectual content of this thesis is the product of my own work, except to the extent that assistance from others in the project's design and conceptions or in style, presentation and linguistic expression is acknowledged.

I HAVE submitted a digital copy of this thesis.

Word count excluding references, tables and captions: …….

(Signed)……Date…….

Thesis committee (names, not signatures):

Supervisor……..Co-supervisor…….

Committee:……..

…….

……..

I am fully aware that the School retains a copy of the thesis and is free to allow them to be consulted or borrowed. The thesis may be restricted for up to 2 years or longer by a written request to the Head of School.

Abstract

In the clay alluvial fields used for irrigated cotton production in the lower Gwydir Valley in northwestern NSW, prior stream channels occupy 15 % of the landscape. These prior stream channels act as significant hydrological features and offer pathways for deep draining water to interact with buried palaeochannels. There is therefore a need to map the connectivity and spatial extent of these features to improve the scientific understanding of the associated hydrological processes. Electromagnetic (EM) instruments, which measure apparent electrical conductivity (σ_a), have been widely used to map the areal distribution of soil properties such as clay content and deep drainage risk, however resolving σ_a with depth has rarely been attempted. The aim of this research was to use a DUALEM-421 to infer the spatial distribution of soil particle size fractions (i.e. sand, silt and clay) and soil properties (i.e. $EC_{1:5}$, CEC and ρ) that relate to σ_a across a prior stream channel in an irrigated cotton field in the lower Gwydir Valley. This was achieved by using three inversion algorithms to estimate the spatial distribution of true electrical conductivity (σ) from the σ_a data. These are *DUALEM-2d* and *DUALEM-3d*, partial solutions and *DUALEM-2d-Full*, full solution to the inversion problem. The spatial distribution of σ from the full solution appears superior in terms of visual representation of the soil profile. Small σ values represent the location of sandy and loamy sediments of a prior stream channel, whilst larger σ values represent the clay soil types across the clay alluvial plain. In addition, the *DUALEM-3d* σ model resolves the spatial distribution of the sediments with depth across the study area. The relationship between the measured soil properties and σ is not significant, therefore further research is needed to achieve better relationships between estimated σ and soil properties.

Acknowledgements

"Knowledge is in the end based on acknowledgement"

– Ludwig Wittgenstein, philosopher.

There are many people I would like to thank for supporting me this year in undertaking my honours project. Firstly, I would like to thank my wonderful supervisor Dr John Triantafilis who was there every step of this journey, from helping me attain a scholarship, to organising the field trip and collecting the DUALEM-421 data and teaching me much about the scientific journey. Equal thanks to visiting academic, Assistant Professor Fernando Santos from the Centro de Geofísica-Instituto Don Luís Laboratório Associado (Universidade de Lisboa) who wrote the inversion programs and who so very patiently answered all my questions about it, even after he had returned to Portugal. There have also been others who have given me invaluable insights regarding the background theory of electromagnetic induction instruments throughout this learning experience. In this regard I would like to thank Associate Professor Bryce Kelly of the School of BEES (UNSW) and Mr Rick Taylor (Principal) of DUALEM. I would also like to acknowledge the Cotton, Catchment and Communities Cooperative Research Centre for providing me with an honours scholarship that funded my field work. I would also like to thank Mr Sean Boland (Irrigation Manager) at Auscott 'Midkin' for allowing me access to Field 11 and providing us with various pieces of equipment to enable us to carry out the DUALEM-421 survey. I also thank Morteza Jami, Don Pagé, Chris Meyers, the students from GEOS3721 and the staff at the BEES office (UNSW) for assistance in laboratory and administrative work. And last, but not at all least, a huge thank you to my family and friends, especially Mum, Martin, Dad, Nic, Leah, Kate and Mick.

Kira Bruzgulis

University of New South Wales (2009)

Note: This thesis has been written in the style of *Geoderma*. A "Guide for Authors" for this Journal can be found at the following website:

http://www.elsevier.com/wps/find/journaldescription.authors/503332/authorinstructions

Table of Contents

Abbreviations

EM	Electromagnetic
HCP	Horizontal coplanar
PRP	Perpendicular
DOE	Depth of exploration
σ_a	Apparent electrical conductivity (mS/m)
σ	True electrical conductivity (mS/m)
CEC	Cation exchange capacity

1. Introduction

In the arid and semi-arid regions of the world, the growth in crop production has largely been facilitated by the introduction of irrigated agriculture. However, in many instances water management is inefficient. This is due to significant water loss in the form of deep drainage, a process whereby water that is not retained in the soil or used by plants passes through the root zone and into the groundwater. In Australia, excess deep drainage across the Riverine Plains of the Murray Darling Basin (Butler et al., 1983) is synonymous with irrigation inefficiencies associated with a network of prior stream channels. These prior stream channels act as significant hydrological features because of their high porosity and permeability, and offer pathways for deep draining water to interact with buried palaeochannels (ancient river deposits).

In the clay alluvial fields used for irrigated cotton production in the lower Gwydir Valley in northwestern NSW, prior stream channels occupy 15 % of the landscape (Needham, 1991). Although many prior stream channels are visible from aerial photographs, at times they are buried beneath the soil and are difficult to locate. In order to improve the scientific understanding of the hydrological processes across this landscape, especially where the management of water is crucial and climatic models and trends suggest that rainfall is in decline (Kothavala, 1999), there is a need for better representation and ability to map the connectivity and spatial extent of prior stream channels and palaeochannels (Triantafilis et al., 2009b).

Due to the time consuming nature of measuring and mapping soil properties with depth and in order to collect information cost-effectively, geophysical techniques are increasingly being used successfully to better discern the soil stratigraphy (Auken et al.,

2006; Pellerin and Wannamaker, 2005). Electromagnetic (EM) induction is a cost effective and proximal geophysical method that has successfully been employed in measuring both the areal (Triantafilis et al., 2001; Triantafilis et al., 2003; Triantafilis et al., 2004) and stratigraphic (Triantafilis et al., 2009b; Vervoort and Annen, 2006) distribution of apparent electrical conductivity (σ_a – mS/m) of prior stream channels in different regions across the Murray Darling Basin.

The σ_a measured by EM instruments is influenced by the true electrical conductivity (σ – mS/m) of different layers within the soil, as well as the physical operating factors of the EM instrument (Callegary et al., 2007; Gomez-Trevino et al., 2002; McNeill, 1980b). The σ of the soil itself is influenced by of a range of soil electrical properties, including amount of soluble salts, clay, cation exchange capacity (CEC) and moisture present in the soil (McNeill, 1980a) making it possible to infer information about these soil properties and others related to them. In order to estimate the σ from σ_a data, mathematical modeling can be employed to obtain 2D or 3D representations of the distribution of σ within a soil profile.

The aim of this study was to use EM imaging and σ_a collected by a DUALEM-421 to infer the spatial distribution of soil properties and soil particle size fractions related to σ_a across a prior stream channel in an irrigated cotton field in the lower Gwydir valley. EM imaging is defined by Christensen (1997) as 'an approximate inverse mapping of data into a model' and is achieved by the inversion of σ_a, using three inversion algorithms to estimate the σ of the soil at discrete increments.

2. Materials and Methods

2.1 Study area

The lower Gwydir Valley is located 500 km north-northwest of Sydney in a semi arid region and is extensively used for irrigated cotton production. A large percentage of this area features the clay alluvial landscape consisting of self mulching clays and non-self mulching clays to transitional red brown earths (Stannard and Kelly, 1968). However, parts of this landscape are associated with prior stream channels characterised by red brown earths and deep sandy soil (Stannard and Kelly, 1968). Red brown earths are generally unsuitable for irrigation farming due to their higher risk in deep drainage (Huckel, 2004; Triantafilis et al., 2003; Vervoort and Annen, 2006). In the lower Gwydir Valley, prior stream channels occur in 15 % of the landscape (Needham, 1991). Fig. 1 shows the soil mapping units of Stannard and Kelly (1968) that exist within the lower Gwydir Valley. The red areas are the red brown earths and deep sandy soils that are associated with prior stream channels.

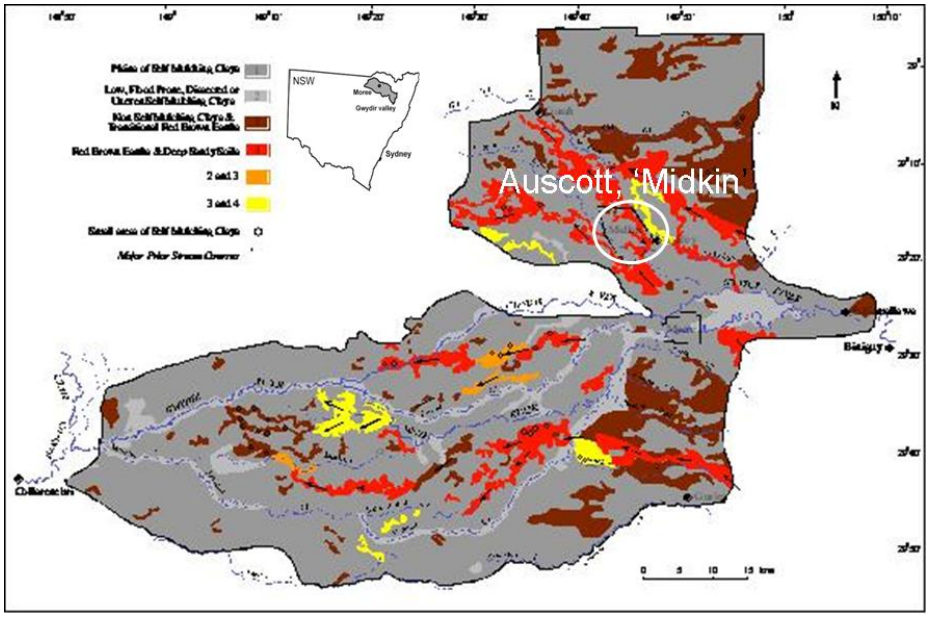

Fig. 1. Soil mapping units of the lower Gwydir Valley and the location of Auscott, 'Midkin' (adapted from Stannard and Kelly, 1968).

The study site is located within Field 11, which covers 244 Ha of Auscott 'Midkin'. 'Midkin' is a large irrigated cotton farm located approximately 20 km northwest of Moree, NSW (Fig. 1). The area is located at the Australian Map Grid (AMG) reference of 6755660 N and 767020 E. Field 11 has a long history of waterlogged conditions, particularly in the central and southwestern parts of the field where the red-brown earths, associated with prior stream channels are apparent (Stannard and Kelly, 1968). Two prior stream channels pass through Field 11. Fig. 2 shows the cross-section of a typical prior stream formation (Fig. 2a) and a terminal branch minor prior stream channel (Fig. 2b). These formations consist of a range of soil horizons, ranging from surface and subsurface horizons of brown sandy loam to sandy clay loams and brown light clays to yellow brown sandy clays (Stannard and Kelly, 1968). Adjacent to these channels and underlying them the subsoil horizons are medium to heavy textured clays (Stannard and Kelly, 1968).

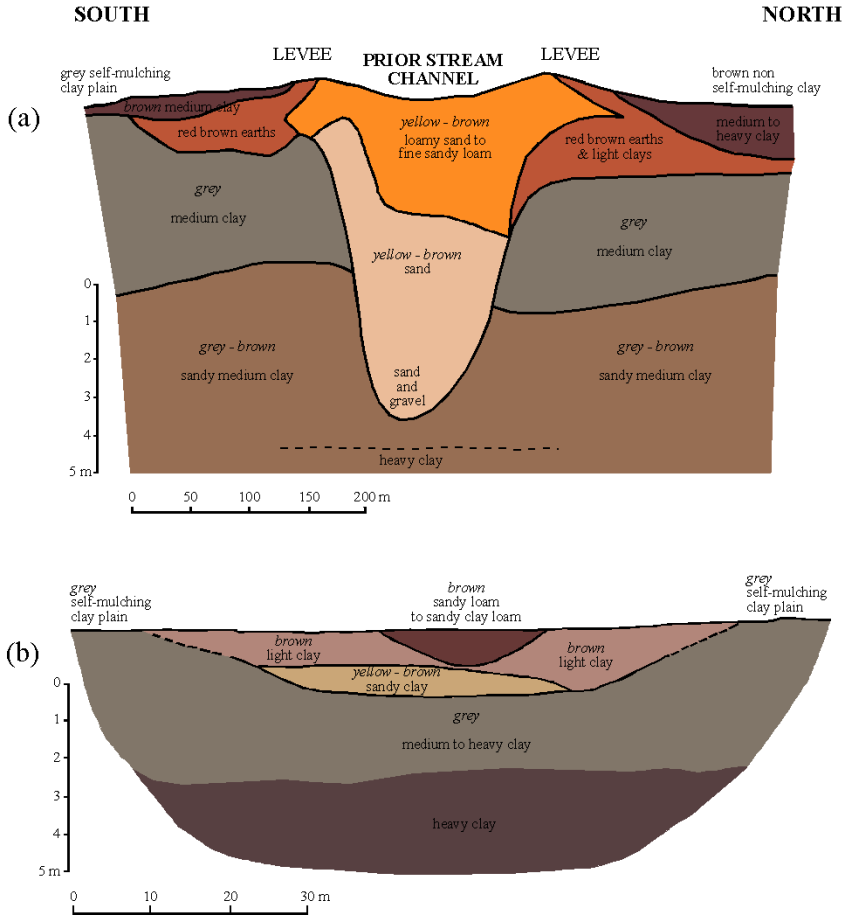

Fig. 2. Cross sections of: a) a typical prior stream channel formation and b)a terminal minor branch prior stream channel (Stannard and Kelly, 1968).

2.2 Instrumentation

The DUALEM-421 (DUALEM Inc., Milton, Ontario, Canada) operates on the principle of EM induction. The DUALEM-421 consists of a single transmitting coil located at one end of the instrument that transmits a continuously varying primary magnetic field at 9.1 kHz which induces eddy currents within the soil. The eddy current induces a secondary magnetic field which is detected by three pairs of receiving coils called dual dipoles, situated 1, 2 and 4 m away from the transmitting coil. The secondary magnetic field is a function of the frequency of operation of the DUALEM-421, the intercoil spacing and the electrical conductivity (σ – mS/m) of the soil (McNeill, 1980b). Each dual dipole consists of two coil arrays, one coil with horizontal windings forming a horizontal coplanar (HCP) array with the receiver and one coil with vertical windings forming a perpendicular (PRP) array.

The DUALEM-421 measures the apparent electrical conductivity (σ_a – mS/m) of the soil, which is a ratio of the primary to secondary magnetic fields. Each of the six coil arrays of the DUALEM-421 respond to the different σ values within different layers of the soil from the surface to a particular depth. This depth is called the depth of exploration (DOE), which depends on the geometry of the coil arrays, including intercoil spacing and orientation. The DOEs of the σ_a measurements of the HCP coil arrays of the DUALEM-421 are 0 to 1.5 m (1mHcon – mS/m), 0 to 3 m (2mHcon – mS/m), 0 to 6 m (4mHcon – mS/m) respectively. The DOEs for the σ_a measurements of the PRP coil arrays of the DUALEM-421 are 0 to 0.6 m (1mPcon – mS/m), 0 to 1.2 m (2mPcon – mS/m) and 0 to 2.4 m (4mPcon – mS/m) respectively (Fig. 3).

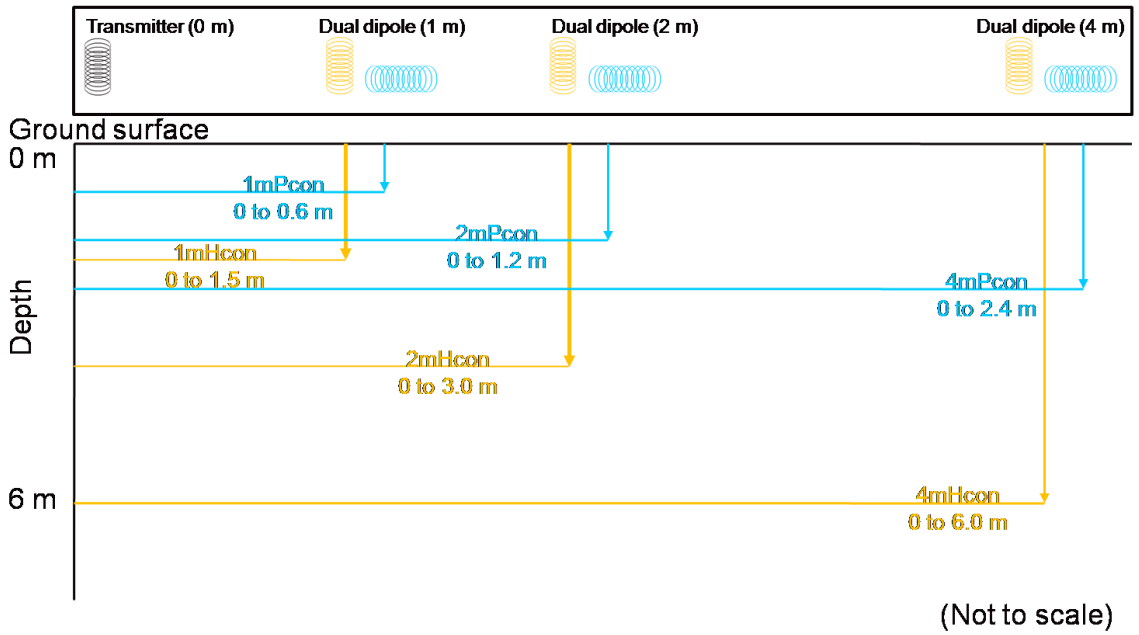

Fig. 3. Schematic of a DUALEM-421 showing the respective depths of exploration (DOEs) of the 1, 2 and 4 m dual dipoles that measure the horizontal coplanar apparent conductivity (σ_a) response (Hcon) and perpendicular σ_a response (Pcon) of the soil (adapted from Dualem, 2008).

Previous EM studies in Field 11 have employed various EM instruments including the Geonics EM-38 and EM-31 (Geonics Inc., Mississauga, Ontario, Canada) and have focused on the lateral distribution of the σ_a across the field (Huckel, 2004; Triantafilis et al., 2001; Triantafilis et al., 2003). These studies have mapped the location of prior stream channels within Field 11. More recently Vervoort and Annen (2006) have aimed to map the vertical distribution of the σ_a of a palaeochannel in the adjacent field to Field 11 (Field 12). Taking into account that prior stream channels have been found to be most distinct from 2 to 7 m (Triantafilis et al., 2009b; Vervoort and Annen, 2006) the DUALEM-421 is a practicable instrument to use in order to carry out a σ_a survey in this field.

2.3 Apparent conductivity (σ_a) data collection

The DUALEM-421 and a NovaTel SMARTV1 antenna was used to provide geo-referencing of the σ_a data collected in the WGS84 format. Subsequently the location data was converted into Northings and Eastings of the Geocentric Datum of Australia (GDA94). The DUALEM-421 and global positioning system (GPS) data were collected using a Holland Scientific GeoSCOUT data logger (GLS-400). The DUALEM-421 was mounted on a mobile frame 0.3 m above the ground surface and attached 5.5 m behind a vehicle. The GPS unit was attached to the roof of a vehicle with a 5.5 m offset from the instrument being accounted for. The σ_a data were obtained along 12 transects. Each transect is approximately 1.1 km long and are spaced 25 m apart. The σ_a from six different DOEs of the DUALEM-421 were collected along each transect with measurements obtained approximately 0.5 m apart. In total 34 038 measurements were made along the 12 transects. The transects are the same as those previously described by Triantafilis et al. (2001), chosen to ensure that the vehicle and mobile frame were aligned in the appropriate traffic lane and to minimise soil compaction which may cause spurious σ_a measurements. As such, they are designated and described in terms of the transect numbers previously used. That is, the eastern most transect is called transect 22 whilst the western most is called transect 16.5 (Fig. 4). The focus of this thesis is on transect 21.5 which is where soil information is available.

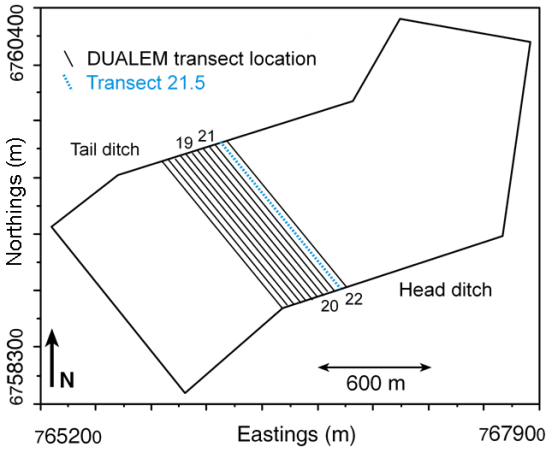

Fig. 4. Location of the DUALEM-421 σ_a survey in Field 11 (transects 16.5 to 22.0), spaced 25 m apart. Transect 21.5 is where soil information is available (adapted from Triantafilis et al., 2001).

2.4 Inversion techniques

The aim of mathematical inversion of σ_a is to obtain an image of the distribution of σ within a soil profile. In soil science our interest is to obtain estimates of σ within the root and vadose zone, e.g. the variation of σ of the topsoil (0 to 0.3 m) can help to characterise the seedbed, and the variation of σ of the subsurface (0.3 to 0.6 m) and subsoil (0.6 to 1.2 m) can help to characterise the subsurface and root zone, respectively. Delineating the vertical variation of σ within these discrete increments from σ_a collected using a DUALEM-421 requires the use of an inversion algorithm. Here the *DUALEM-2d, DUALEM-2d-Full* and *DUALEM-3d* inversion programs were employed. All three algorithms are modified versions of the nonlinear smoothness constrained inversion algorithm described in Santos (2004) and incorporate a damping factor (the Lagrange parameter) that is used to control the balance between the data fit and its closeness to the initial model. It is important to take note that the inverse problem is an ill-posed one. Ill-posed behaviour is a fundamental feature of many inverse problems due to the smoothing of data that occurs in the process of the calculation (Aster et al., 2005).

The input file for the algorithms includes the σ_a data from the DUALEM-421 (i.e. 1mHcon, 1mPcon, 2mHcon, 2mPcon and 4mHcon and 4mPcon σ_a measurements), the height of the instrument above the ground surface, as well as each data point's Easting, Northing and elevation. An iterative process allows the final model to be obtained.

2.4.1 DUALEM-2d

The initial earth model used in the *DUALEM-2d* inversion process is made up of a 2D mesh of hexahedral blocks distributed according to the locations of measurement sites and coil spacing from the DUALEM-421. *DUALEM-2d* consists of a 1-dimensional (1D) inversion with 2-dimensional (2D) smoothness constraints between adjacent 1D models. The algorithm is based on the cumulative function which is a mathematical function of depth. The cumulative function describes the relative contribution to the secondary magnetic field, measured at the receiver of the DUALEM-421 due to the homogeneous material within a thin horizontal layer at a depth (Callegary et al., 2007; Gomez-Trevino et al., 2002; Kaufman and Keller, 1983; McNeill, 1980b). In the presence of a layered-earth model, the relative contribution to the secondary magnetic field from all material up to a depth below the sensor can be expressed by the cumulative function (for HCP or PRP configurations) as defined by McNeill (1980b) and Wait (1962).

In order to estimate the σ of the soil it is important to understand the relationship between the measured σ_a data and the instrument response. The DUALEM-421 operates such that the σ_a of the soil is linearly proportional to the response of the instrument when operating under certain conditions (known as operation at low induction numbers – LIN) explained in detail by McNeill (1980b) and Wait (1962). Under these circumstances interpretation of σ_a data is a relatively simple task. However, in highly conductive terrains, such as the clay alluvial fields of the lower Gwydir Valley, the σ_a measurements are no longer linearly proportional to the instrument response, making the interpretation of σ_a more complicated. In this situation, there is a certain σ_a value where this non-linearity begins to occur which is intrinsic to each coil array for the DUALEM-421, specifically referred to in the DUALEM-421 manual (Dualem, 2008). In the scope of this study the use of the cumulative function to calculate the model response (σ) means that the instrument response at each of the constituent

model blocks is not being considered. This is a major limitation of the *DUALEM-2d* program.

2.4.2 DUALEM-2d-Full

The initial earth model used in the *DUALEM-2d-Full* inversion process is the same as the one described for *DUALEM-2d*. *DUALEM-2d-Full* is based on the inverse procedure with a non-linear model explained in detail by Hendrickx et al. (2002) and Aster et al. (2005). It is important to note that the limitation of the nonlinear relationship between the measured σ_a data and the instrument response does not exist in the *DUALEM-2d-Full* program. The program uses the full solution of the inductive phenomena in a layered earth which takes into account the nonlinearity between the measured σ_a data and the instrument response. Therefore, the models calculated by this program should represent the σ distribution more realistically (Santos, 2009).

2.4.3 DUALEM-3d

The initial earth model used in the *DUALEM-3d* inversion process is a 3-dimensional (3D) mesh of hexahedral blocks distributed according to the locations of the measurement sites and coil spacings of the DUALEM-421. This technique represents a 1D spatially constrained approach and the final model is a rough representation of a 3D model (i.e. quasi-3D model). *DUALEM-3d* is also based on the cumulative function and is therefore limited by the nonlinearity of the relationship between σ_a and the instrument response.

2.5 Soil sampling and laboratory analysis

Soil calibration data from 17 soil sampling sites were collected along transect 21.5 and used for calibration of the σ_a data collected with the DUALEM-421. At each sampling site, a soil core was collected to a depth of 1.5m and bulked into 0.30 m increments. The soil samples were analysed to determine clay, silt and sand particle size fractions using the hydrometer method (Gee and Bauder, 1979) and the electrical conductivity of a 1 part soil to five part water extract ($EC_{1:5}$ - dS/m). The cation exchange capacity (CEC-cmol(+) kg^{-1}) was determined using the Tucker (1974) method with a mechanical leaching device (Holmgren et al., 1977).

The soil texture (e.g. heavy clay, medium clay, light clay) was determined by considering the Australian Soil Texture Triangle and the three particle size fractions. Soil texture groups are then assigned for each sample, whereby 6 – clay, 5 – light Clays, 4 – clay loams and 3 – loams). Bulk density (ρ – g/cm^3) is estimated using the model that was developed by Rhoades et al. (1976). Fig. 5 shows the locations of the sample sites along transect 21.5. The sites are numbered from 1 through to 17, from south to north.

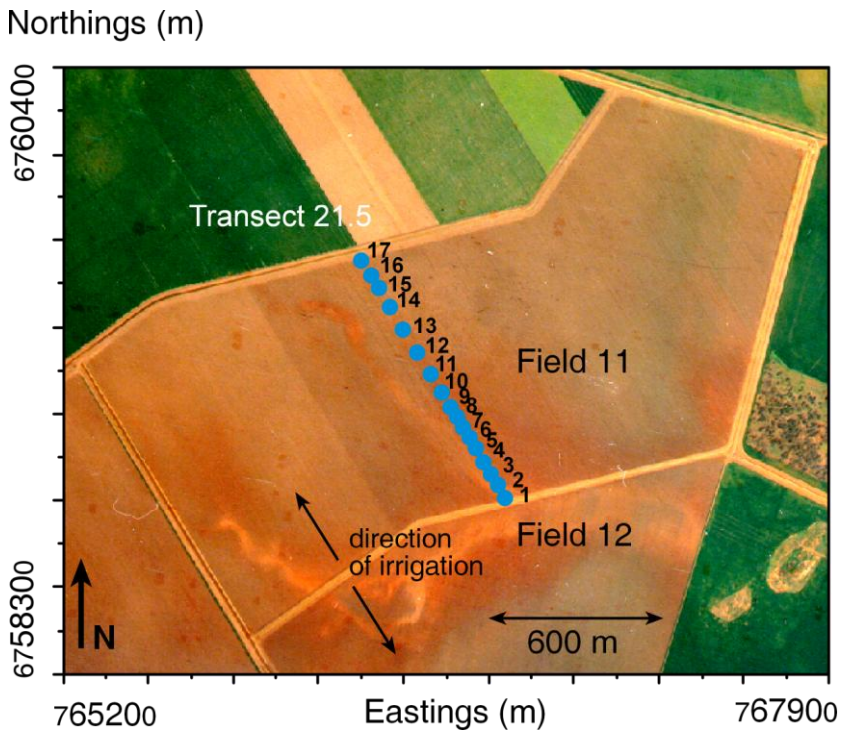

Fig. 5. Locations of soil sampling sites labeled 1 to 17 along transect 21.5.

3. Results and Discussion

3.1 Apparent conductivity (σ_a) data

Fig. 6 shows the 1mHcon and 1mPcon σ_a data (Fig. 6a), the 2mHcon and 2mPcon σ_a data (Fig. 6b) and the 4mHcon and 4mPcon σ_a data (Fig. 6c) from the DUALEM-421, as well as the elevation (Fig. 6d) along transect 22.0. With respect to the smallest coil spacing, it is evident that north of the Northing of 6759125 the larger 1mHcon σ_a and 1mPcon σ_a represent the clay alluvial plain (Fig. 6a). Conversely, south of the Northing of 6759125 the smaller 1mHcon and 1mPcon σ_a values represent the prior stream channel which extends approximately 200 m in width. Given that the DOE of the 1mHcon σ_a measurement is deeper (0 to 1.5 m) as compared to the shallow DOE of the 1mPcon σ_a (0 to 0.6 m), this suggests that the surficial 0 to 0.6 m of the soil profile may be smaller in σ than the subsurface (0.6 to1.2 m).

Fig. 6b shows that the σ_a data collected with the 2 m coil spacing is similar in terms of the pattern of σ_a distribution. The major difference is that the 2mHcon and 2mPcon σ_a are approximately 2 times larger than the equivalent data from the 1 m coil spacing. This suggests that the σ is larger within the shallow vadose zone (1.2 to 3 m).

The data from the 4 m coil spacing is also similar to that measured with the 1 and 2 m coil arrays in terms of the spatial pattern of σ_a (Fig. 6c). However, both the 4mHcon and 4mPcon σ_a are equivalent to each other along the entire transect. Taking into consideration that the 4mHcon and 4mPcon σ_a values are influenced by the σ of the layers within the soil profile between 0 to 6 m and 0 to 2.4 m respectively, this suggests that between depths of 2.4 to 6 m the σ of the soil may be smaller and therefore may not influence the instrument response to the extent which a layer of larger σ might. Also of note, the 4mHcon σ_a values

show that it is evident that the presence of the prior stream channel is still significant at a depth of 6 m with respect to the trough located in the southern part of the transect.

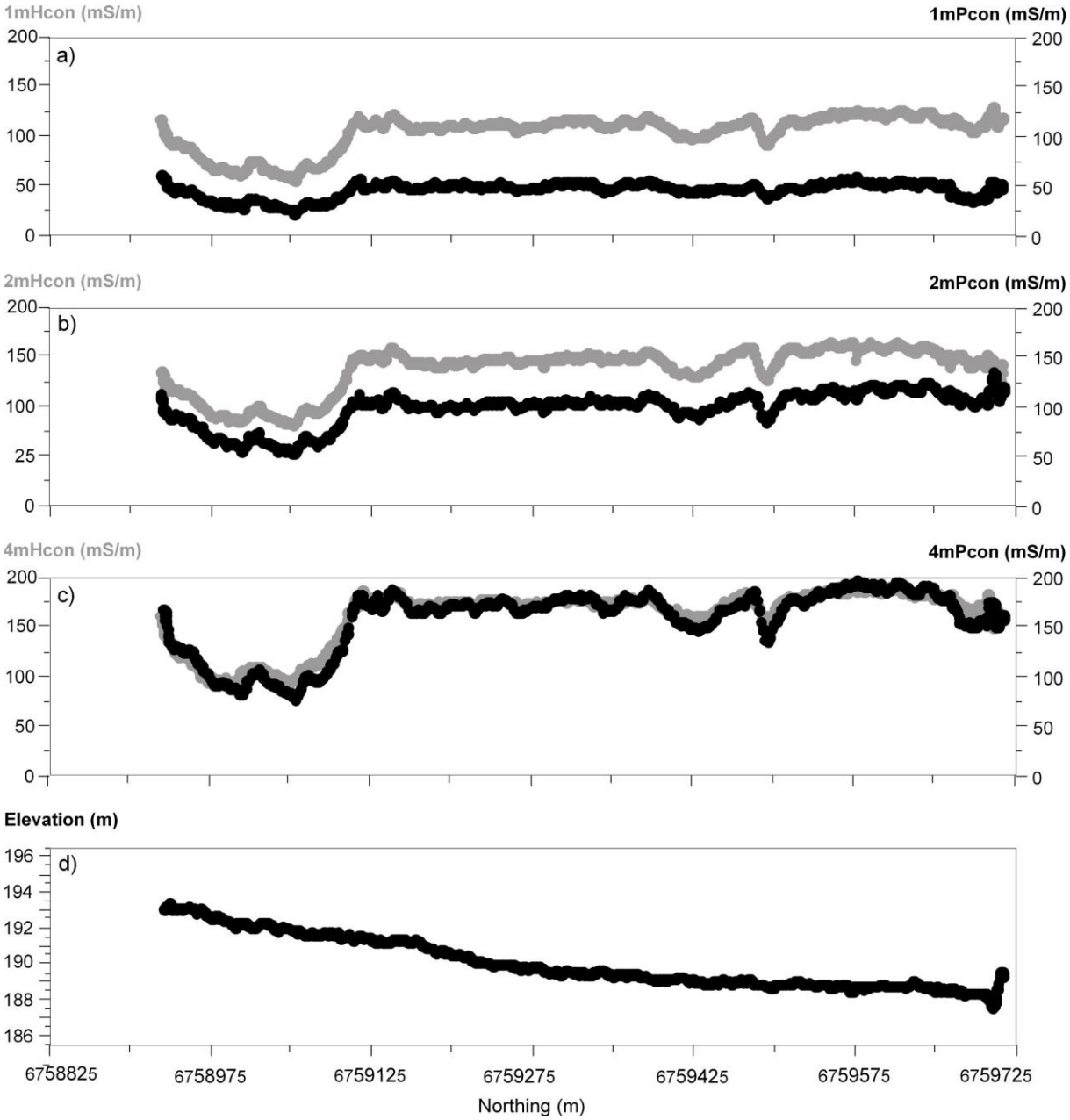

Fig. 6. Spatial distribution of apparent soil electrical conductivity (σ_a - mS/m) along transect 22.0 measured using a DUALEM-421 in horizontal coplanar (Hcon) and perpendicular (Pcon) modes of operation, and intercoil spacings of: a) 1m, b) 2m; and, c) 4m, and d) altitude (ASL - m).

Fig. 7 shows the 1mHcon and 1mPcon σ_a data (Fig. 7a), the 2mHcon and 2mPcon σ_a data (Fig. 7b) and the 4mHcon and 4mPcon σ_a data (Fig. 7c) from the DUALEM-421, as well as the elevation (Fig. 7d) along transect 21.5. Fig. 7a, b and c show that the general pattern of

the distribution of σ_a is similar to the data from the equivalent coil spacings in transect 21.5, in terms of the contrast of the prior stream channel and the clay alluvial plain. It is also worth taking into consideration that a number of smaller or minor prior stream channels may exist in transect 21.5 indicated by the small σ_a troughs located near Northings of 6759275 and 6759500 along the central part of the transect.

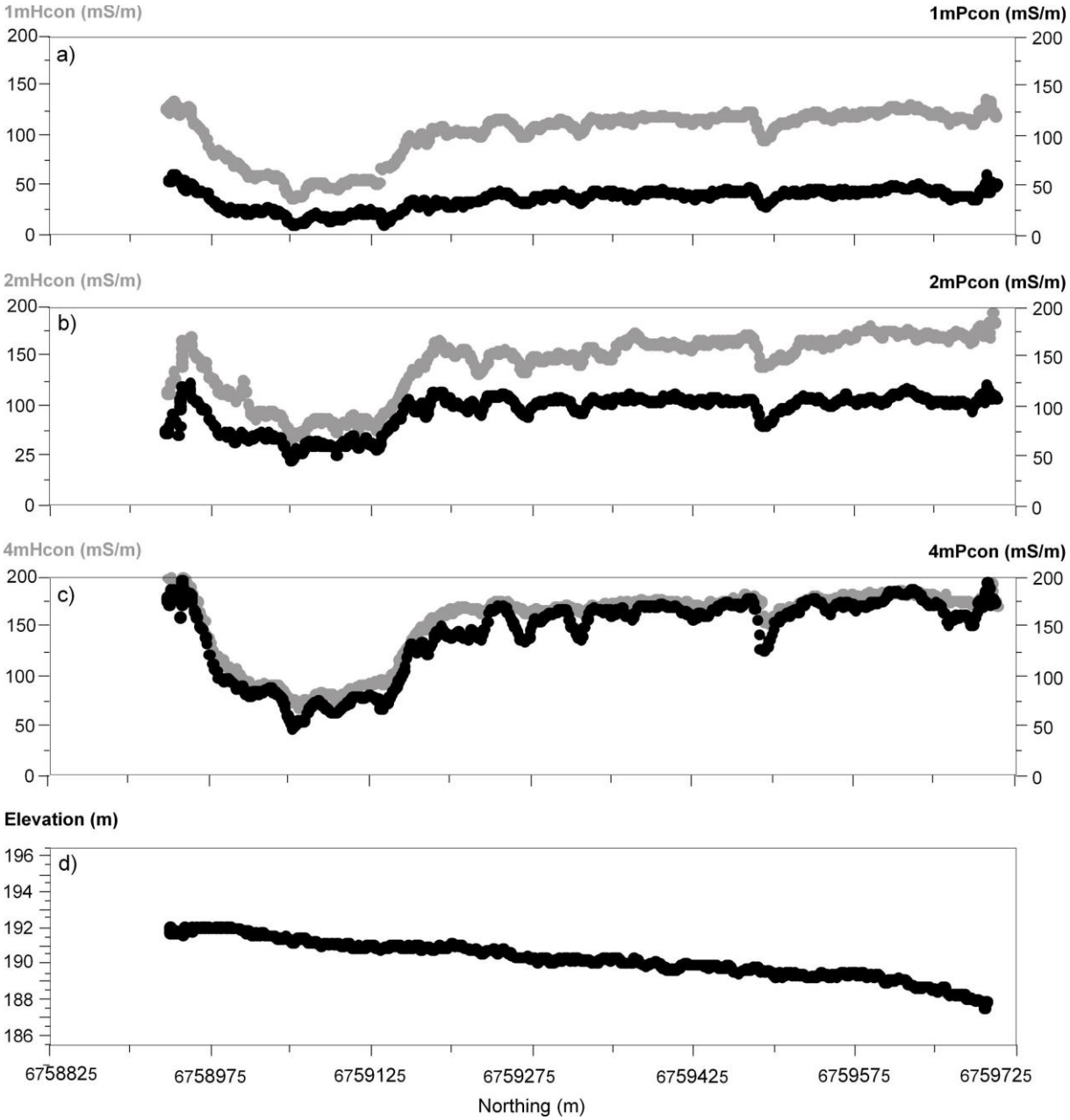

Fig. 7. Spatial distribution of apparent soil electrical conductivity (σ_a - mS/m) along transect 21.5 measured using a DUALEM-421 in horizontal coplanar (Hcon) and perpendicular (Pcon) modes of operation, and intercoil spacings of: a) 1m, b) 2m; and, c) 4m, and d) altitude (ASL - m).

Fig. 8 shows the 1mHcon and 1mPcon σ_a data (Fig. 8a), the 2mHcon and 2mPcon σ_a data (Fig. 8b) and the 4mHcon and 4mPcon σ_a data (Fig. 8c) from the DUALEM-421, as well as the elevation (Fig. 8d) along transect 21.0. A similar pattern of σ_a data is once again observed. The areal extent of the prior stream channel here is the widest, measuring approximately 275 m extending from a Northing of 6758975 to 6759275.

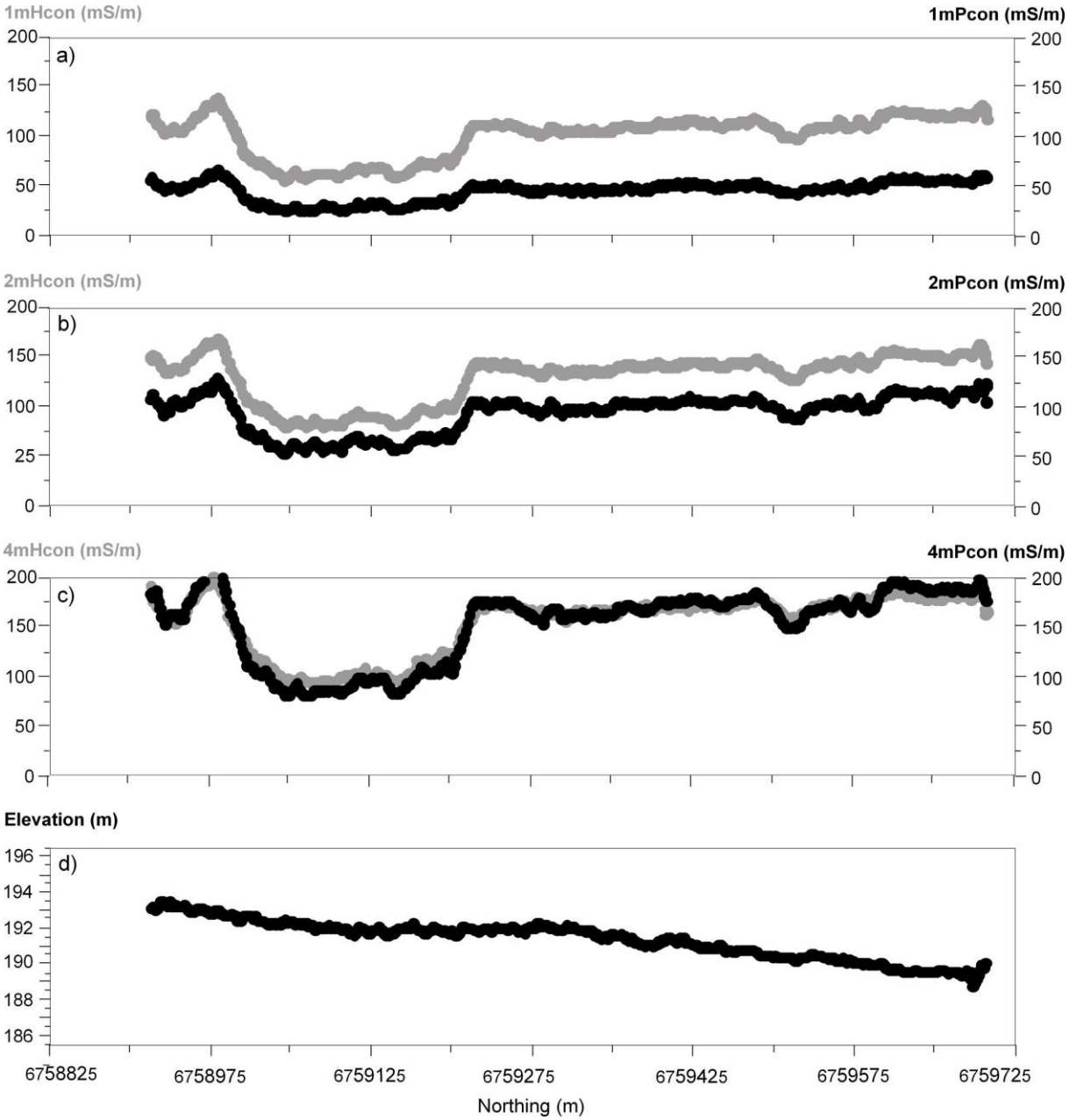

Fig. 8. Spatial distribution of apparent soil electrical conductivity (σ_a - mS/m) along transect 21.0 measured using a DUALEM-421 in horizontal coplanar (Hcon) and perpendicular (Pcon) modes of operation, and intercoil spacings of: a) 1m, b) 2m; and, c) 4m, and d) altitude (ASL - m).

Fig. 9 shows the 1mHcon and 1mPcon σ_a data (Fig. 9a), the 2mHcon and 2mPcon σ_a data (Fig. 9b) and the 4mHcon and 4mPcon σ_a data (Fig. 9c) from the DUALEM-421, as well as the elevation (Fig. 9d) along transect 20.5. The major difference here is the location of the prior stream channel. It measures approximately 125 m in width and is situated between Northings of 6759125 and 6759275. This indicates that the position of the prior stream channel extends towards the north relative to its position in transect 21.5.

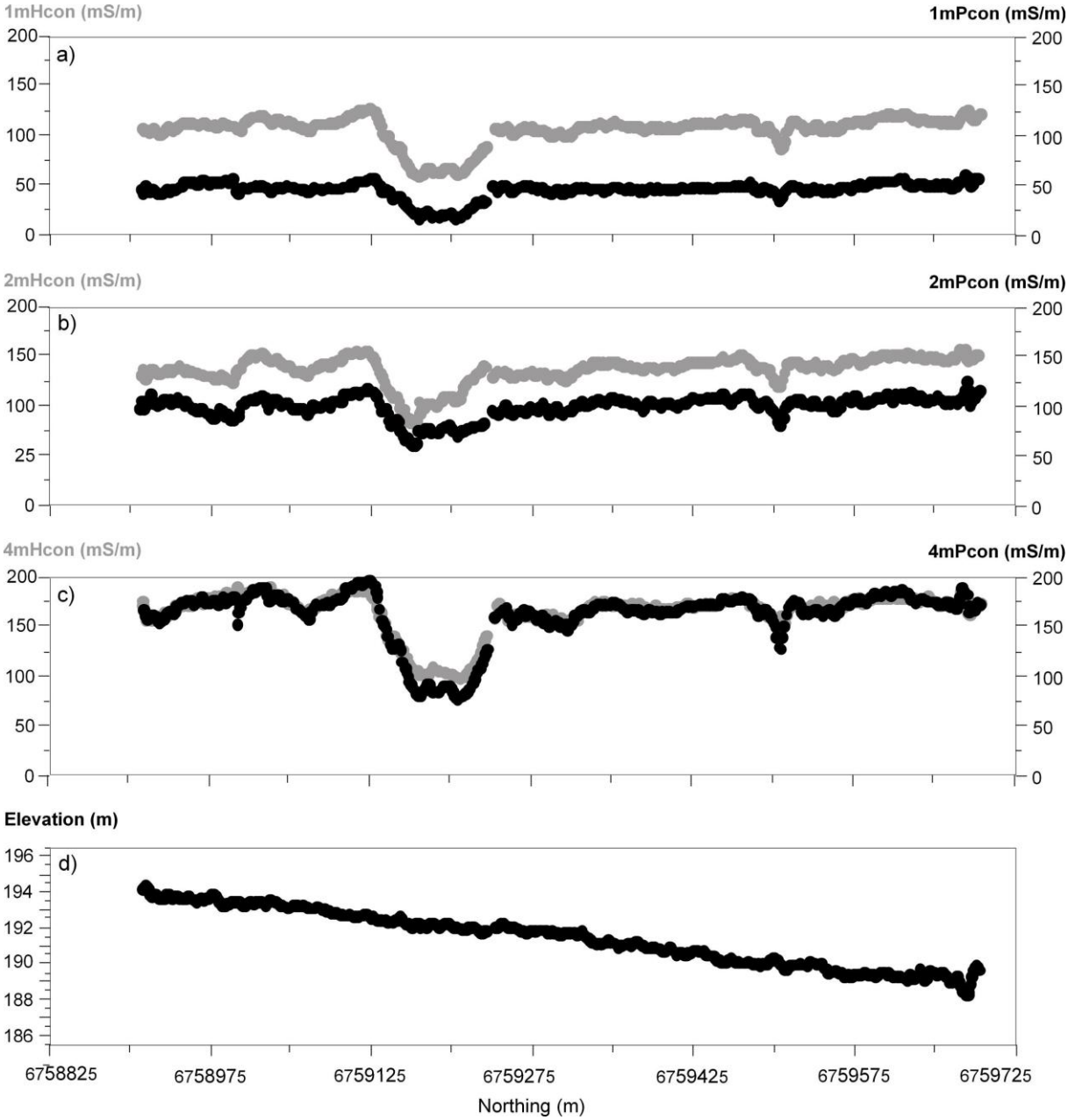

Fig. 9. Spatial distribution of apparent soil electrical conductivity (σ_a - mS/m) along transect 20.5 measured using a DUALEM-421 in horizontal coplanar (Hcon) and perpendicular (Pcon) modes of operation, and intercoil spacings of: a) 1m, b) 2m; and, c) 4m, and d) altitude (ASL - m).

In order to better appreciate the location and areal extent of the prior stream channel within these transects, Fig. 10 shows 6 maps that have been generated in a grid of 25x25 m from the collected σ_a data using a kriging interpolation method. Fig. 10a and b show the 1mHcon and 1mPcon σ_a respectively, Fig. 10c and d show the 2mHcon and 2mPcon σ_a respectively and Fig. 10e and f show the 4mHcon and 4mPcon σ_a respectively from the data collected along transects 22.0 to 16.5 (east to west). In the centre of the study site, the prior stream channel, represented by the smaller σ_a values (< 100 mS/m) extends from the southeast where it is very well defined in terms of width, to the northwest where it begins to dissipate. Also, the surficial layer (0 to 0.6 m) of smaller σ_a (< 70 mS/m) is represented well by the 1mPcon σ_a in Fig. 10b. With respect to the σ_a values in the root zone (0 to 1.2 m) represented by the 2mPcon σ_a (Fig. 10d) the clay alluvial plain surrounding the prior stream channel is well represented by the increase of σ_a values (100 to 150 mS/m). The σ_a values are the largest (150 to >200 mS/m) from the 2mHcon measurements (Fig. 10c) suggesting the shallow vadose zone (1.2 to 3 m) has the largest σ. Conversely, the σ_a appears to decrease (< 200 mS/m) in the deeper vadose zone (up to 6 m) represented by the 4mHcon σ_a (Fig. 10e).

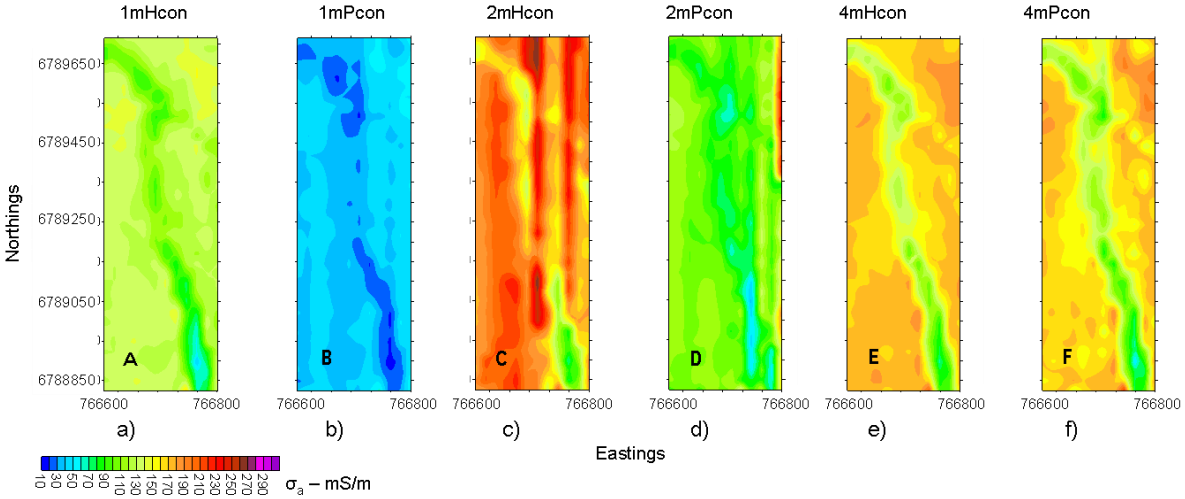

Fig. 10. Maps of interpolated apparent conductivity (σ_a - mS/m) acquired across transects 22.0 to 16.5 (east to west) using a DUALEM-421 in horizontal coplanar (Hcon) and perpendicular (Pcon) modes of operation, for intercoil spacings of: a, b): 1m, c, d): 2 m and e, f): 4 m.

3.2 Spatial distribution of soil particle size fractions and soil properties

Fig. 11a shows the location and depth of the soil sampling sites situated along transect 21.5. Fig. 11 also shows the 2D contour plots of the particle size fractions of clay (Fig. 11b), silt (Fig. 11c) and sand (11d). In general and with respect to the finer textured soil of the clay alluvial plain, it is evident that clay content is larger in the central and northern end of the transect. This is consistent with the larger σ_a values obtained with the DUALEM-421. Conversely, as shown in the southern end of the field the prior stream is characterised by sediments with larger sand content (45 to > 50 %).

At soil sample location 5, the smaller clay content (< 35 to < 40 %) collected indicates the location of the centre of a prior stream channel (Fig. 11b). Further evidence for this is shown in Fig. 11c which shows this part of the transect features larger sand content (< 35 to <45 %) and in Fig. 11d which shows larger silt content (40 to >50 %). These are soil properties that pertain to prior stream channel formations (Stannard and Kelly, 1968). Similar soil properties are also observed to a lesser extent between soil sample locations 14 and 15 and at a depth of approximately 0.9 m. Given that these particle size fractions are equivalent, it can be concluded that a small and buried prior stream channel exists in this location. Conversely, the soil that surrounds the minor buried prior stream channel consists of large clay content (< 40 to >50 %), small silt content (< 40 to <35 %) and small sand content (< 25 to < 15 %) (Fig. 11b, c and d respectively).

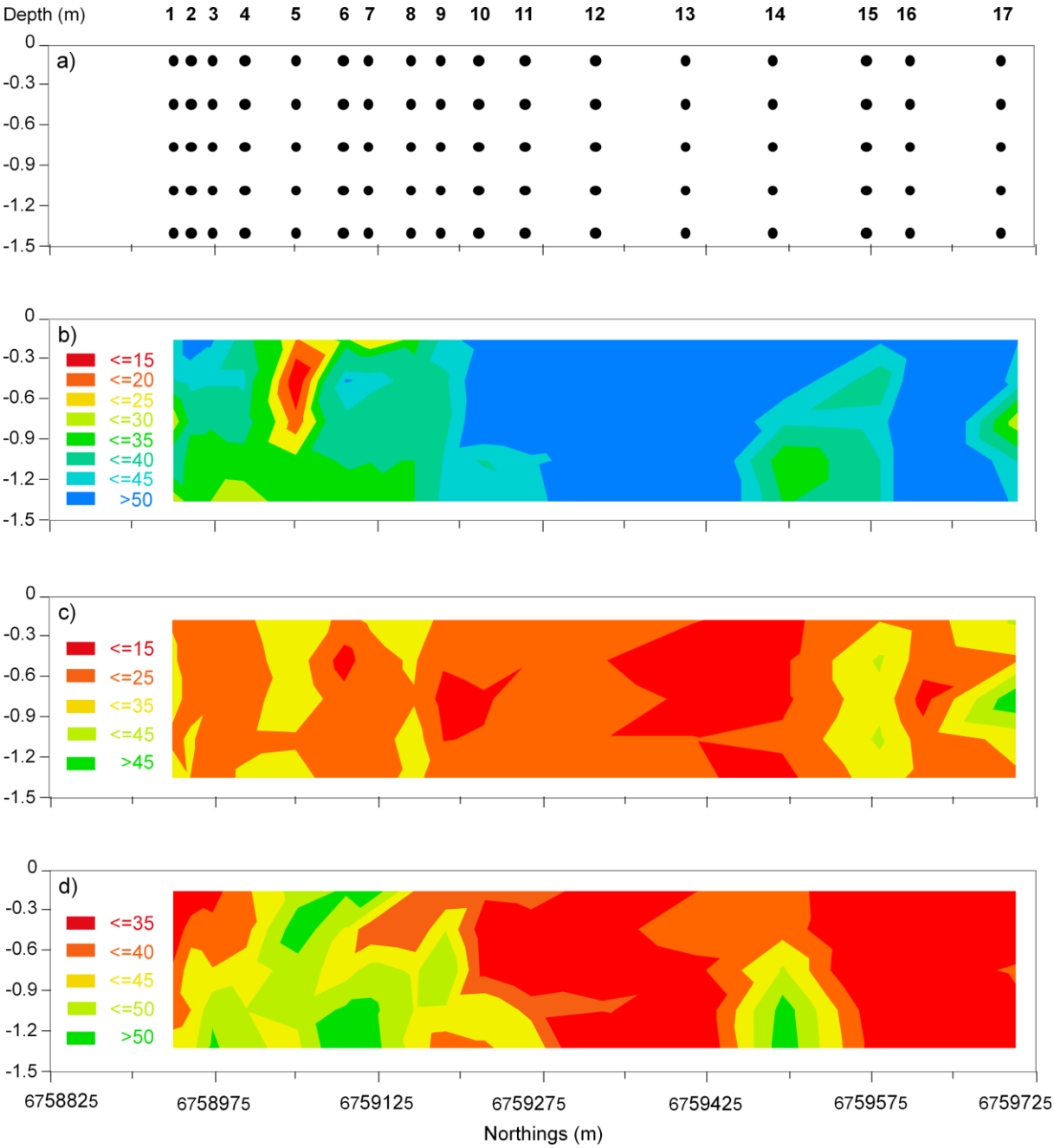

Fig. 11. a) Location and depth of soil sampling across transect 21.5, and 2-dimensional contour plots of the particle size fractions of b) clay (%), c) silt (%) and d) sand (%).

Fig. 12 shows 2D contour plots of soil texture (based on soil texture classes, whereby 6 – clay, 5 – light clays, 4 – clay loams and 3 – loams) (Fig. 12a), the estimated bulk density (ρ – g/cm^3) of the soil (Fig. 12b), the electrical conductivity of 1 part soil and 5 parts water extract ($EC_{1:5}$ – mS/m) (Fig. 12c) and cation exchange capacity (CEC – cmol (+)/ kg) (Fig. 12d) along transect 21.5. The particle size distribution in Fig. 11b, c and d is reflected by the soil texture and ρ contour plots as shown in Fig. 12a and b respectively. The uniform loam to clay loam profile of the prior stream channel adjacent to the uniform clay profile of the clay alluvial field is interspersed with sections of stratification (Fig, 12a). This is particularly evident at soil sample locations 6 and 7, and as such suggests a gradual transition from the prior stream channel to the clay alluvial plain. The ρ is large (< 1.40 to > 1.45 g/cm^3) in the location of the prior stream channel compared to that of the clay alluvial plain (< 1.40 to < 1.30 g/cm^3) (Fig. 12b). This indicates that the soil of the prior stream channel has less structure and is composed of single grains, a property exhibited by soil that is loamy in nature. Conversely, the soil in the clay alluvial plain is more likely to be composed of peds, reflecting the clay nature of a soil with medium to heavy clay, evident in the self mulching and non-self mulching clays of the alluvial plains in the lower Gwydir Valley. Furthermore, this reflects the structural aggregation expected in the soil texture classes presented in Fig. 12a.

Fig. 12c shows that the smaller $EC_{1:5}$ values (< 0.75 mS/m) correspond to the parts of the transect where the prior stream channels are located. Given that these sections of the soil profile consist of loamy soil with larger silt and sand content, any soluble salts present will drain through the soil profile when it is irrigated. In addition, between soil sample locations 8 to 14 the surficial soil layer (0 to 0.6 m), which has smaller $EC_{1:5}$, overlies larger $EC_{1:5}$ values (< 1.25 to > 2.25 mS/m) that correspond to the clay alluvial plain. This, coupled with the knowledge of the irrigation and salinity history of this region (Stannard and Kelly, 1968),

suggests that the $EC_{1:5}$ values are derived from primary salinity within and below the root zone (0.9 to 1.5 m).

With respect to the distribution of CEC along transect 21.5, the larger CEC pertaining to the clay alluvial plain is evidently larger than that of the prior stream channel (Fig. 12d). This reflects the pattern of the soil particle size fraction information, specifically the clay content as shown in Fig. 11b, the soil texture information as shown in Fig. 12a and also the ρ as shown in Fig. 12b as expected.

With respect to the σ_a measurements from transect 21.5, the soil information collected to a depth of 1.5 m within the soil profile influences the 1mHcon and 1mPcon σ_a measurements due to their respective DOEs (i.e. 0 to 0.6 m and 0 to 1.5 m) (Fig. 7a). Specifically, the clay content (Fig. 11b), the $EC_{1:5}$ (Fig. 12c) and the CEC (Fig. 12d) should directly influence the σ within the different layers of the soil. Of particular note, the small 1mPcon σ_a values (~0 to 50 mS/m) do not coincide with the large clay content or finely textured soil shown in Fig. 11b and Fig. 12b however, they do coincide with a smaller $EC_{1:5}$ and CEC measurements within this depth of the soil profile as shown in Fig. 12c and d. It is worth noting that the study site has not been irrigated for more than 4 years and coupled with being located in a semi arid region, a lack of rainfall and water within the subsoil (0 to 0.6 m) may be attributable to the smaller σ_a measurement of the 1mPcon σ_a data. With respect to the 1mHcon σ_a, the general pattern of the prior stream channel in the south adjacent to the clay alluvial plain in terms of clay content, ρ, $EC_{1:5}$ and CEC is apparent.

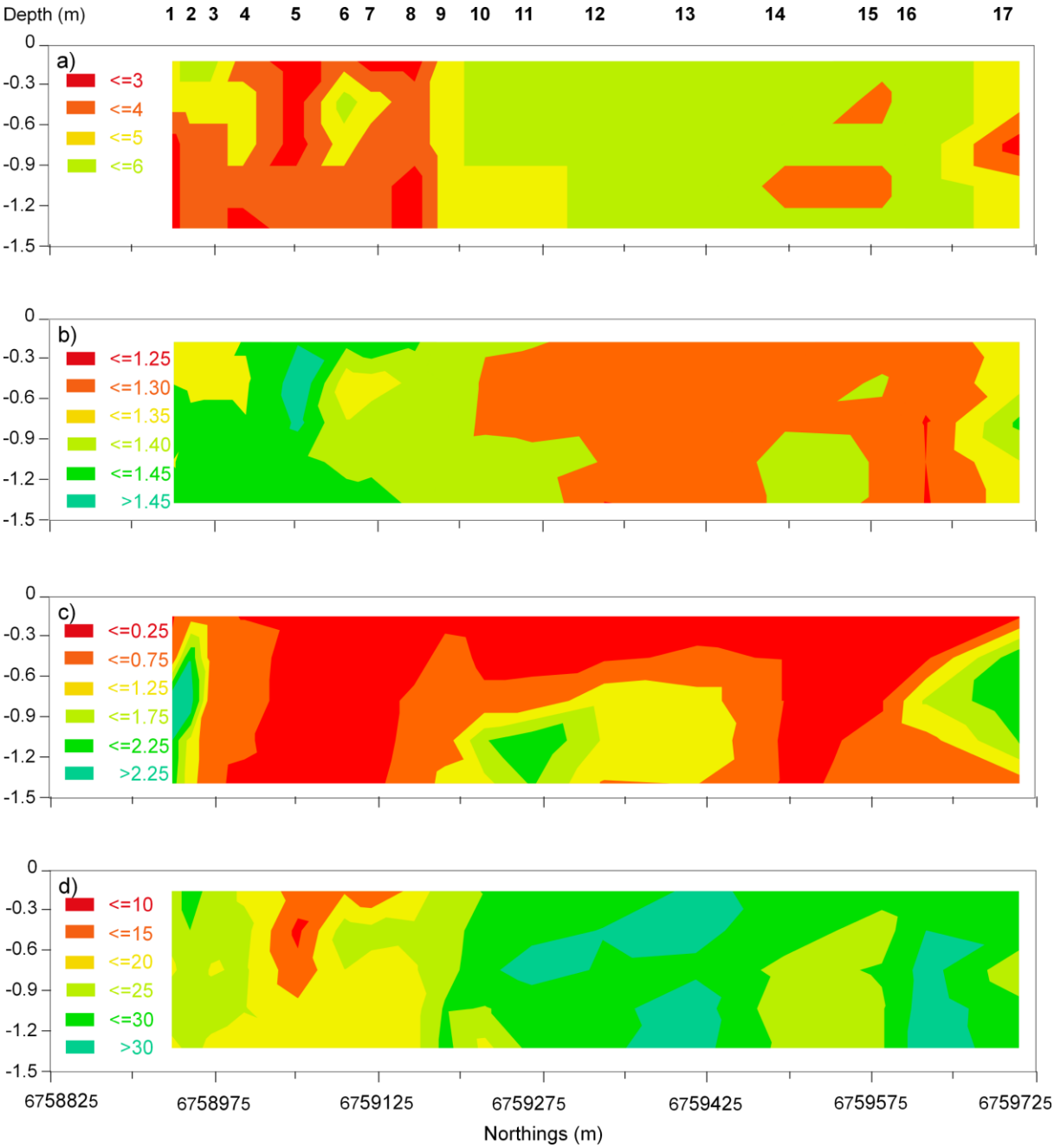

Fig. 12. 2-dimensional contour plots of a) soil texture (based on soil texture classes, whereby 6 – Clay, 5 – Light Clays, 4 – Clay Loams and 3 – Loams), b) estimated bulk density (ρ – g/cm^3), c) electrical conductivity of 1 part soil and 5 parts water extract ($EC_{1:5}$ – mS/m) and d) cation exchange capacity (CEC – cmol (+)/ kg) along transect 21.5.

In addition and with respect to the deeper sediments in the general area of the study site, soil data collected by Vervoort and Annen (2006) in the adjacent field to Field 11 (Field 12) show similar evidence for a prior stream channel. In this study a 370 m transect was established from the edge of Field 12 across a buried palaeochannel between Eastings of 766500 and 766800. Fig. 13 shows 2D contour plots of particle size fractions of clay (Fig. 13a), gravel (Fig. 13b) and sand (Fig. 13c) along this transect to a depth of 12.5 m obtained from 13 soil cores along the transect (Vervoort and Annen, 2006). Interestingly, the larger σ_a measurements obtained by the 2 m and 4 m dual dipoles of the DUALEM-421 generally coincide with the pattern of clay content present in the deeper sediments in this soil profile (Fig. 7b and c). In addition the larger sand content present from 8 to 12 m deep suggests the presence of a buried palaeochannel. Triantafilis et al. (2009a) suggested that when the sand content of the vadose zone (up to 6 m) is high (> 40 %), the sediments may represent the location of a palaeochannel. A palaeochannel is also suggested at this depth by the large gravel content (10 to 50 %) (Fig. 13b).

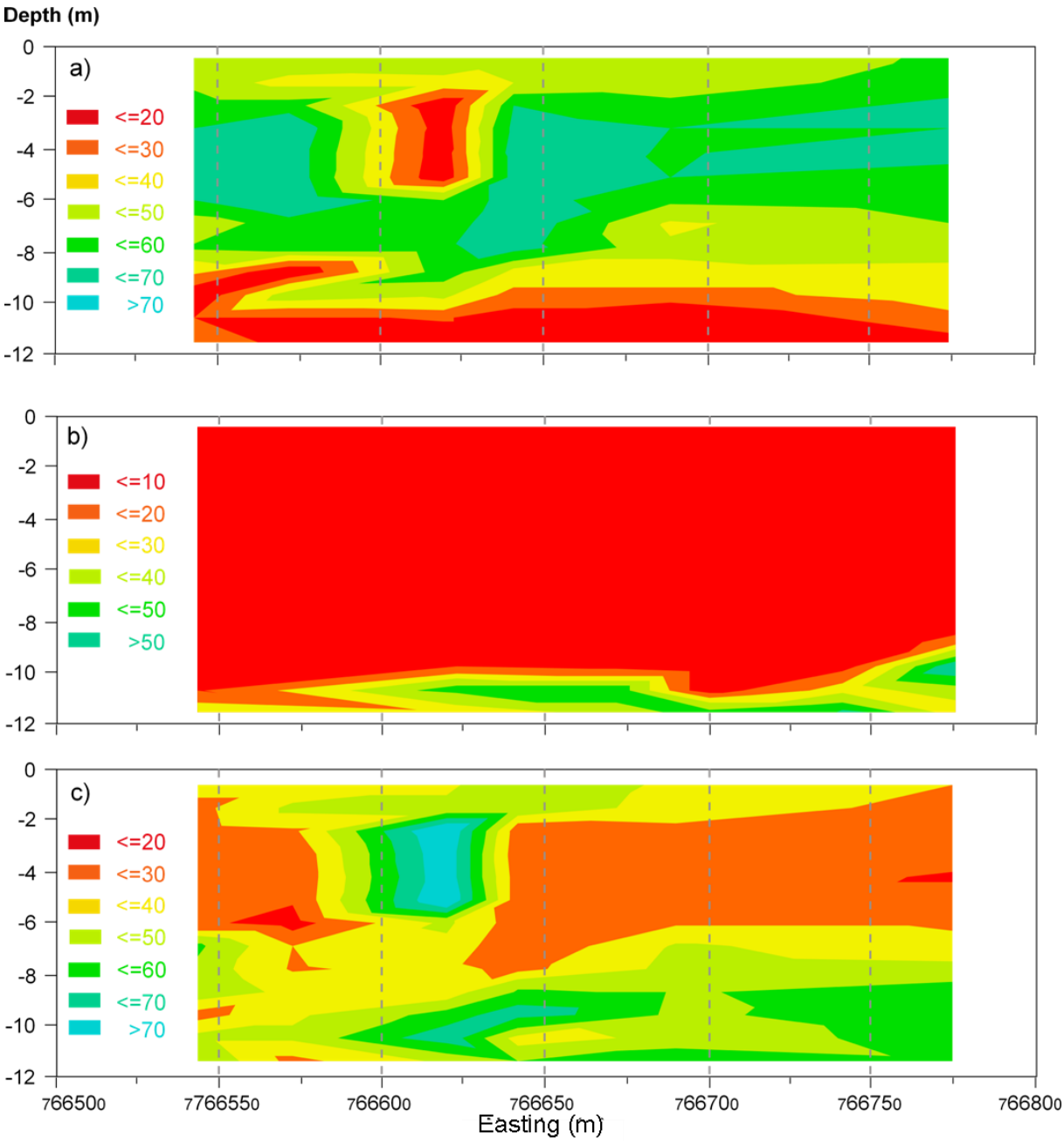

Fig. 13. 2-dimensional contour plots of particle size fractions of a) clay (%), b), gravel (%) and c) sand (%) along a transect located across a buried palaeochannel in Field 12, adjacent to Field 11 (Vervoort and Annen, 2006).

3.3 Profile reconstruction using DUALEM-2d

Fig. 14 shows the spatial distribution of σ generated by the *DUALEM-2d* inversion program for transect 22.0 (Fig. 14a), transect 21.5 (Fig. 14b), transect 21.0 (Fig. 14c) and transect 20.5 (Fig. 14d). The σ models for these transects were obtained by inverting the measured σ_a data and using a damping factor of 0.1. The average global misfit for all models is 5.85 %. It is evident that the overall subtle stratigraphic elements of the landscape are well represented by these inversion models. With respect to the lateral distribution of soil types, it is evident that the layers of larger σ (300 to > 400 mS/m) pertaining to the clays that dominate the clay alluvial landscape are discerned from the layers of smaller σ (< 100 mS/m) which pertain to the prior stream channel. Considering the root zone (0 to 1.2 m) of all models, a layer of small σ (< 100 mS/m) from approximately 0 to 1 m in the soil profiles is apparent. The pattern here is not equivalent to the clay content information shown in Fig. 9a. This may be attributed to the small 1mPcon σ_a measurements (Fig. 6a) caused most likely by the lack of moisture in the topsoil from 0 to 0.6 m.

With respect to Fig. 14a, the extent of the prior stream channel between Northings of 6758900 and 6759125 is evident. The small σ (< 100 mS/m) represents the sandy to loamy soil of the prior stream channel. This is the most defined section of the prior stream channel in terms of width in the study site and it is located in the vicinity of the head ditch, which is the main water supply canal for irrigation in Field 11. The coexistence of the widest section of the prior stream channel and the head ditch implies that inefficiency in irrigation is problematic in this area of the field. North of this location in the central and northern end of the transect and at a depth of approximately 2 to 3 m, the larger σ (> 200 mS/m) that occurs in a thin layer of highly conductive sediment underlies the surficial sediment of small σ. This could be attributed to higher clay content within the shallow vadose zone (up to 3 m).

Considering the vadose zone (> 3 m) in the northern part of transect 22.0, sediments of smaller σ ($\leq$ 100 to < 200 mS/m) underlie the thin layer of highly conductive sediment, suggesting the presence of a buried palaeochannel which is plausible, given the soil particle size information presented in Fig. 13a, b and c. A similar σ pattern is observed for transects 21.5, 21.0 and 20.5 (Fig. 14b, c and d). In addition, the position of the prior stream channel extends towards the north in each successive transect, relative to its position in transect 22.0.

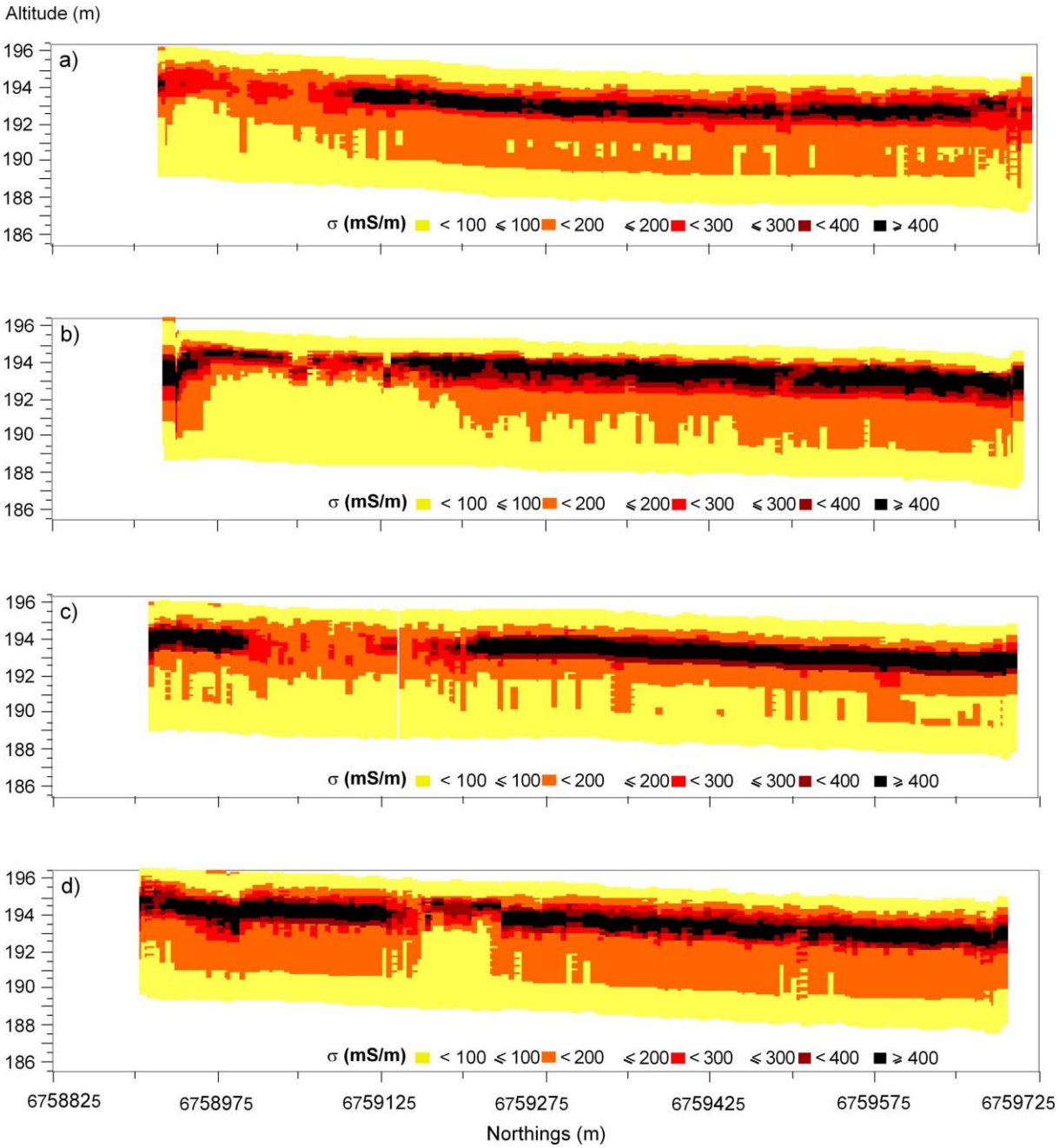

Fig. 14. 2-dimensional (2D) spatial distribution of soil electrical conductivity (σ - mS/m) obtained from *DUALEM-2d* and σ_a data along: a) transect 22.0, b) transect 21.5, c) transect 21.0, and d) transect 20.5.

3.4 Profile reconstruction using DUALEM-2d-Full

Fig. 15 shows the spatial distribution of σ generated from the *DUALEM-2d-Full* inversion program for transect 22.0 (Fig. 15a), transect 21.5 (Fig. 15b), transect 21.0 (Fig. 15c) and transect 20.5 (Fig. 15d). The σ models for these transects were obtained by inverting the measured σ_a data and using a damping factor of 0.1. The average global misfit for all models is 5.68 %. Generally, a similar pattern is observed in the σ models shown in Fig. 15, compared to those in Fig. 14 in terms of the clay alluvial plain adjacent to the prior stream channel and the surficial layer of small σ (< 100 mS/m). The major difference is the physiography portrayed within the soil profile is distinctly different in terms of σ distribution. With respect to Fig. 15a and considering the deeper root zone and shallow vadose zone (1 to 3 m) in the central and northern end of transect 22.0, a layer of medium σ ($\leq$ 100 to < 200 mS/m) overlies a highly conductive layer of soil approximately 3 m thick (from 3 to 6 m). This thick, highly conductive layer is not present in the σ model generated by the *DUALEM-2d* program which suggests that the *DUALEM-2d-Full* inversion program responds better to the deeper σ within the soil. The thick, highly conductive layer suggests an increase in clay content or the presence of salts due to primary salinity that occurs naturally below the root zone within this landscape.

Given that the *DUALEM-2d-Full* algorithm is not limited by the nonlinear relationship between the σ_a data and the instrument response and considering the soil property information collected by Vervoort and Annen (2006) as shown in Fig. 12, the σ model generated using *DUALEM-2d-Full* shows a more realistic interpretation of the σ within the transects. This is particularly evident when considering the general physiography of a prior stream channel as shown in Fig. 2a. The different layers of σ that exist below the surficial 1 m of the σ models generally resolve the range of soil horizons present in a typical prior stream channel formation. The range of soil horizons, including surface and subsurface horizons of brown

sandy loam to sandy clay loams likely to be characterised by smaller σ values (<100 to 200 mS/m), and brown light clays to yellow brown sandy clays likely to be characterised by intermediate σ values (200 to 300 mS/m) surrounded by subsoil horizons consisting of medium to heavy textured clays likely to be characterised by larger σ values (300 to > 400 mS/m) are resolved well. However, considering the soil particle size fraction information to a depth of approximately 5 to 6 m collected by Vervoort and Annen (2006) (Fig. 13), coupled with the σ models obtained, the combined information suggests that the prior stream channel is connected to a palaeochannel through sandy to loamy sediments located within the deeper vadose zone (> 6 m). Interestingly this is not the case that was presented by Stannard and Kelly (1968) who suggested that the loamy sands to sand and gravel sediments present in the prior stream channel stop abruptly and overlay medium to heavy clays.

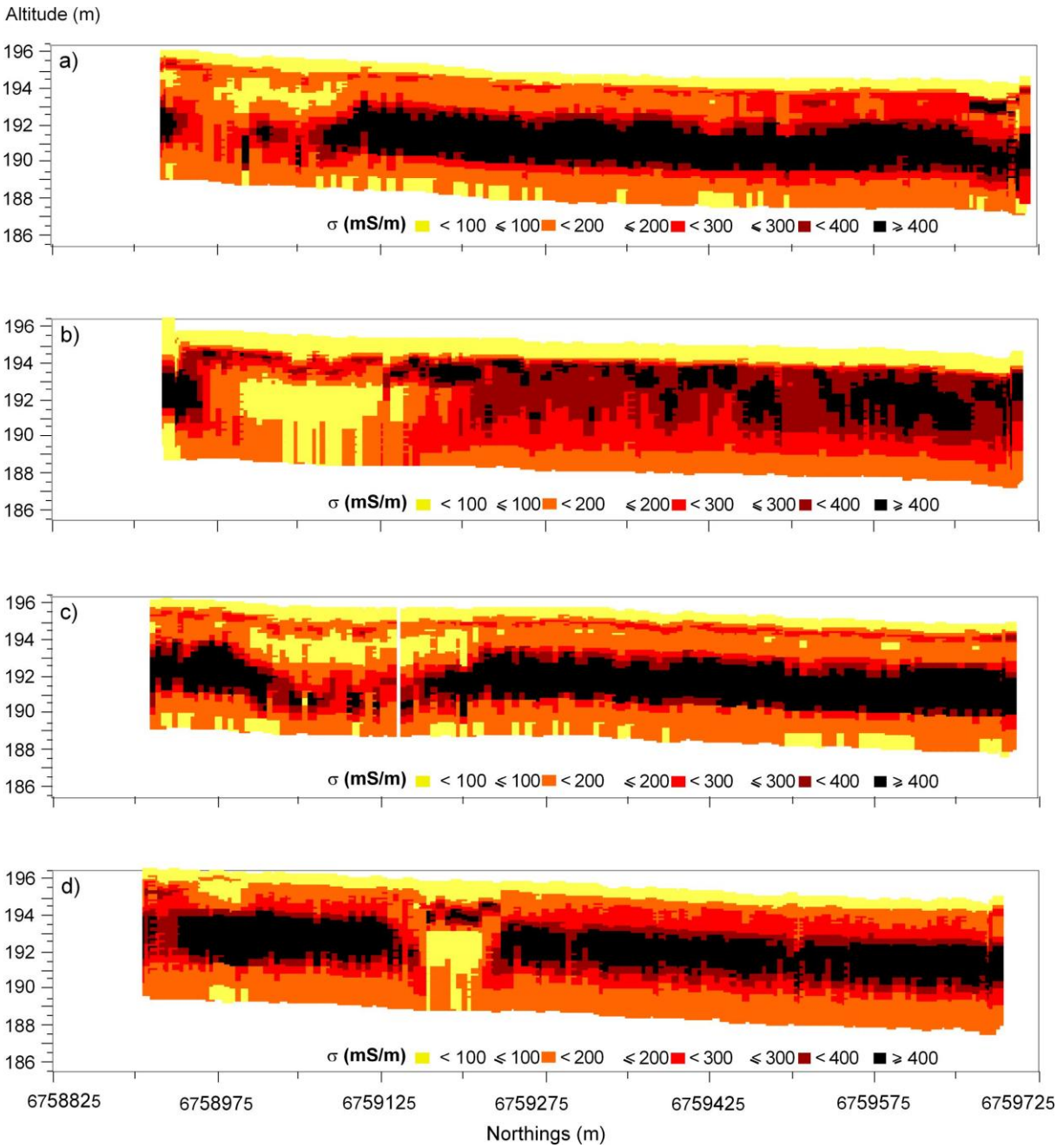

Fig. 15. 2-dimensional (2D) spatial distribution of soil electrical conductivity (σ - mS/m) obtained from *DUALEM-2d-Full* and σ_a data along: a) transect 22.0, b) transect 21.5, c) transect 21.0, and d) transect 20.5.

3.5 Profile reconstruction using DUALEM-3d

Fig. 16 shows the quasi-3D σ model in 4 horizontal slices for 4 depths (0.3, 1, 2, and 4 m). The quasi-3D σ model was obtained by inverting the measured σ_a data from all 12 transects (22.0 to 16.5) using the *DUALEM-3d* program with a damping factor of 0.8. The global misfit is 20 % which is mainly due to the large misfit observed from the 2mHcon σ_a data. Of note, it is important to take into account that the quasi-3D σ models is limited by the non-linearity problem of the cumulative function and therefore may not represent the distribution of σ in a realistic way. Nevertheless, the highly variable nature and the stratigraphic elements of the alluvial landscape are well represented. In general, the pattern of the prior stream channel extending from southeast to northwest through the centre of the study site is evident.

With respect to the first layer (0.3 m) of the quasi-3D σ model, the smaller σ values ($\leq$ 100 mS/m) characterise a similar pattern that has been observed in the σ models from both the *DUALEM-2d* and *DUALEM-2d-Full* inversion programs. The prior stream channel and the surrounding clay alluvial plain can barely be distinguished from each other which may be attributed to the very small σ_a values collected by the 1mPcon measurements from the DUALEM-421. The prior stream channel becomes more apparent in the second layer of the quasi-3D σ model (1 m). With respect to the third layer at 2 m, the distribution of σ in the clay alluvial plain is the largest at this depth (300 to 500 mS/m), which is similarly shown by the thin layer of large σ in the models generated by *DUALEM-2d* (Fig. 14). Conversely, the prior stream channel appears more distinct at the southern end of the study site, indicated by the smaller σ values (< 150 mS/m) and starts to dissipate half way along the study site, indicated by the intermediate σ values (250 to 300 mS/m). The fourth layer of the quasi-3D σ model (4 m) features smaller σ values (100 to 250 mS/m), suggesting the deeper sediments are comprised of a sandy to loamy soil. Furthermore, this may suggest the presence of a

palaeochannel at this depth, similarly to what is observed at this depth in the σ models generated from the *DUALEM-2d* inversion program.

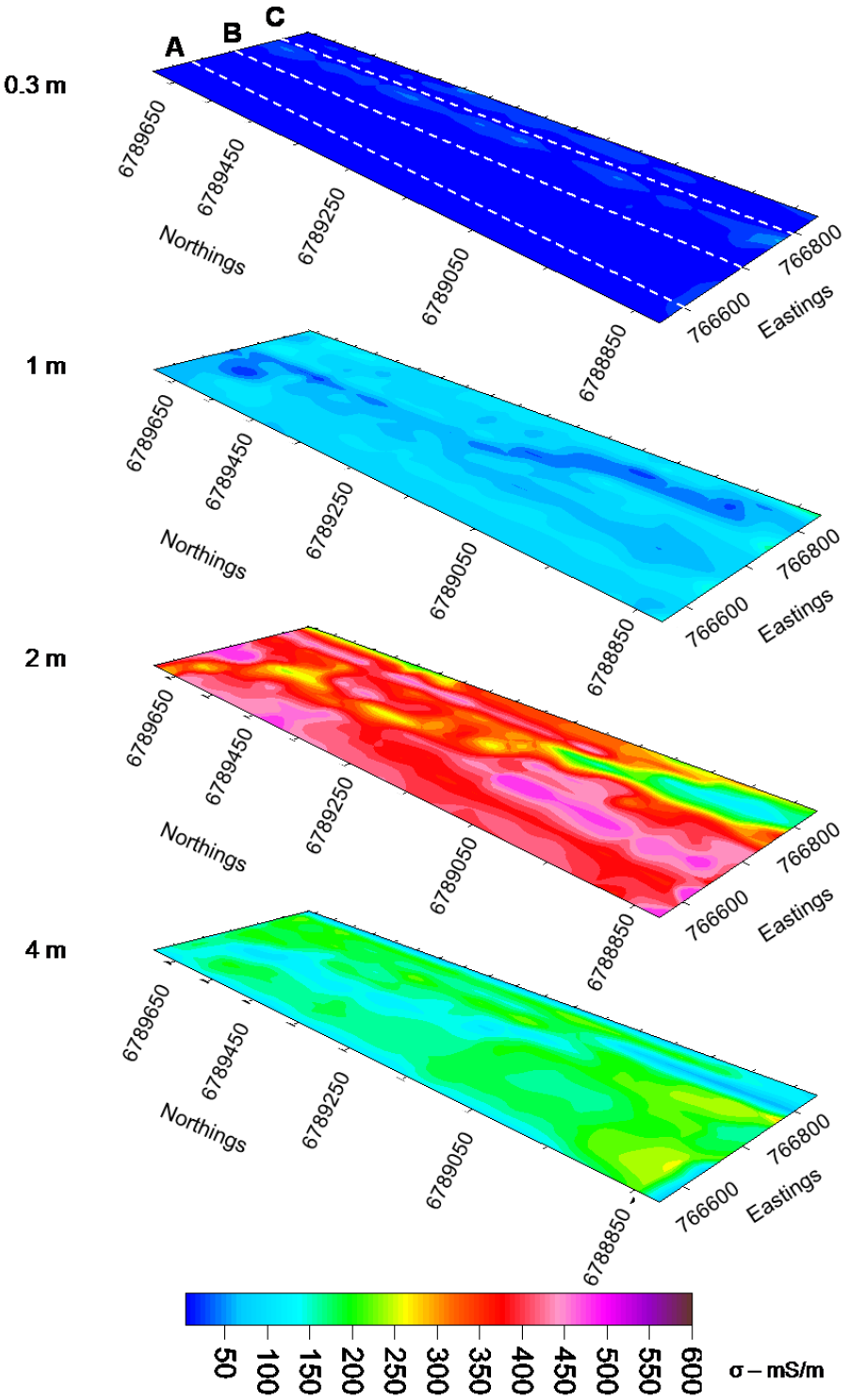

Fig. 16. Horizontal slices at 4 depths (0.3, 1, 2 and 4 m) of the quasi-3-dimensional (3D) spatial distribution of soil electrical conductivity (σ - mS/m) model obtained from *DUALEM-3d* and σ_a data covering transects 22.0 to 16.5. The dashed lines in the top layer represent vertical cross sections along 3 profiles (A, B and C).

Fig. 17 shows the vertical cross sections along the 3 profiles (profiles A, B and C) that are indicated on the surface layer of 3D σ model in Fig. 16. These vertical cross-sections correspond closely to some of the σ models produced from the *DUALEM-2d* program. Specifically, profile A (Fig. 17a) approximately corresponds to transect 17.0 (check) (Fig. B2c, Appendix B), profile B (Fig. 17.b) approximately corresponds to transect 19.5 (Fig. B1b, Appendix B) and profile C (Fig. 17c) approximately corresponds to transect 21.0 (Fig. 14c). These cross sections show an almost identical pattern of a surficial layer of small σ overlying the prior stream channel adjacent to the prior stream channel with small σ in the deeper vadose zone to that obtained with the *DUALEM-2d* inversion program. Once again the prior stream channel extends from the northeast to southwest, where it dissipates in width. In addition, profile B shows two areas of small σ are evident in the centre and northern end of the transect. This formation may pertain to two adjacent prior stream channels, which suggests that the prior stream channel diverges at this part of the transect.

With respect to profile C (Fig. 17c), the general distribution of σ reflects the soil calibration data collected along transect 21.5 (Fig. 12) in terms of $EC_{1:5}$ and CEC measurements (Fig. 12c and d). Specifically, the small σ at the southern end of profile C and the surficial layer corresponds to the smaller $EC_{1:5}$ and CEC measurements in the upper 1.5 m of the soil profile. Conversely, the large σ in the central and northern end of profile C corresponds to the larger CEC measurements in the same location (Fig. 12d). With respect to the particle size fraction data collected by Vervoort and Annen (2006), profile C generally reflects the pattern of clay and sand data shown in Fig. 13 a and c, respectively. Specifically, below a depth of approximately 2 m, small σ values in profile C reflect the large sand content in Fig. 13c and below a depth of 1 m, large σ values reflect the larger clay content as shown in Fig. 13a.

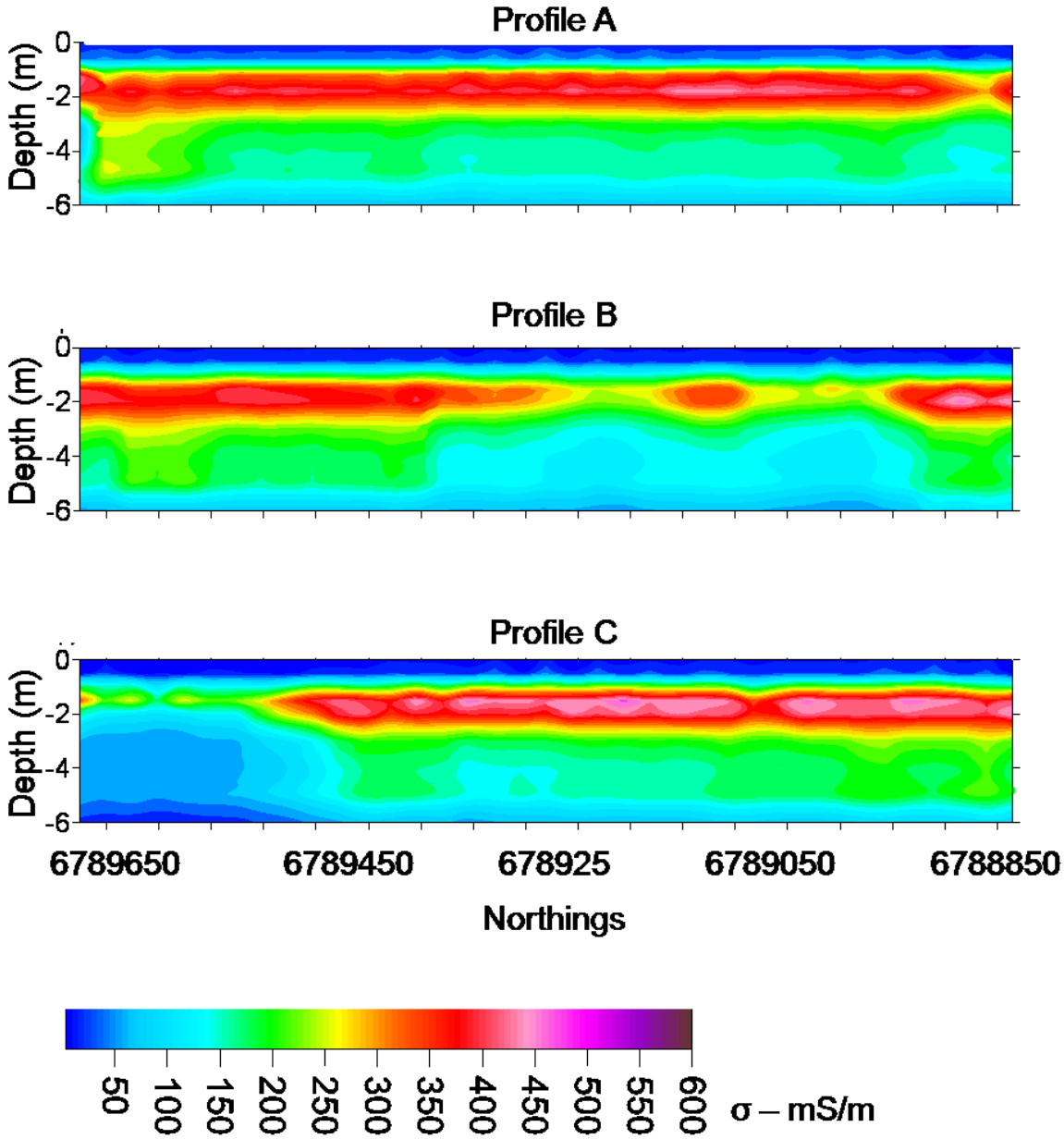

Fig. 17. Vertical cross sections along 3 profiles (A, B and C) from the quasi-3D electrical conductivity (σ - mS/m) model obtained from *DUALEM-3d* and σ_a data from transects 22.0 to 16.5.

3.6 Prediction of soil properties from conductivity (σ) models

Fig. 18 shows six correlation plots of the σ from the models obtained from the *DUALEM-2d* and *DUALEM-2d-Full* programs, respectively versus: clay content (Fig. 18a and b); $EC_{1:5}$ (Fig. 18c and d); and CEC (Fig. 18e and f) collected along transect 21.5. Whist the σ models of transect 21.5 are able to generally represent the adjacent soil types of the prior stream channel and the clay alluvial plain, the potential to use σ to predict clay content, $EC_{1:5}$ and CEC is limited, as shown in the lack of a significant correlation between the σ and different soil property data. The Pearson correlation coefficients (r) for the σ (*DUALEM-2d)* versus clay content, $EC_{1:5}$ and CEC were 0.08, 0.27 and 0.19, respectively. The r values for the σ (*DUALEM-2d-Full)* versus clay content, $EC_{1:5}$ and CEC were 0.08, 0.26 and 0.19, respectively. In the case of the σ models obtained from the *DUALEM-2d* program, the potential for prediction may be limited by the nonlinearity of the cumulative function that the algorithm is based upon. *DUALEM-2d-Full* takes into account the nonlinearity problem, however this does not produce better correlation between σ and soil properties. This could be attributed to the layer of small σ values that exist in the upper 1 m of soil in all the σ models which may reflect the lack of soil moisture in the topsoil at the time of the σ_a survey. If this is the case, in retrospect, all soil samples should have been analysed for moisture content, which was not possible due to time and financial constraints at the time of the investigation.

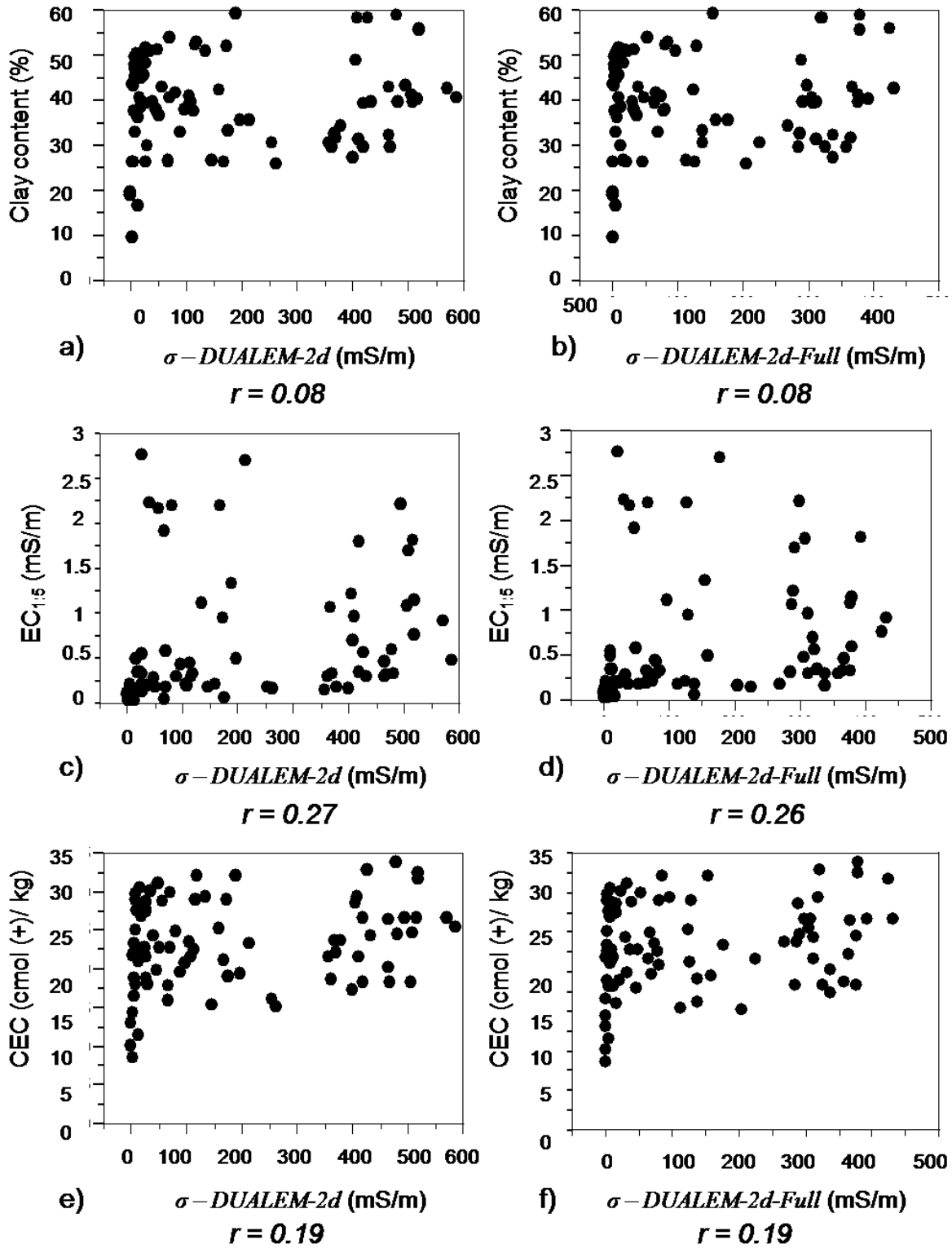

Fig. 18. Correlation plots and Pearson correlation values (r) of electrical conductivity (σ - mS/m) obtained from *DUALEM-2D* and *DUALEM-2d-Full* (respectively) versus: a, b) clay content (%); c, d) electrical conductivity of 1 part soil and 5 parts water extract ($EC_{1:5}$ – mS/m); and e, f) cation exchange capacity (CEC – cmol (+)/ kg) for soil samples obtained along transect 21.5.

4. Conclusions

The spatial distribution of properties within a prior stream channel and clay alluvial plain can be inferred from the true electrical conductivity (σ) generated from the inversion of DUALEM-421 σ_a data collected along 12 transects located within an irrigated cotton growing field in the lower Gwydir valley. With respect to the DUALEM-421 σ_a data, the larger 1mHcon as compared with the 1mPcon σ_a data suggests that the topsoil and subsurface σ is smaller than subsoil σ. The intermediate DUALEM-421 σ_a data, which provides information about the shallow vadose zone, supports this notion because the 2mHcon and 2mPcon σ_a is approximately 1.5 and 2 times larger than the respective σ_a of the 1m measurements. This suggests that clay content, $EC_{1:5}$ or soil moisture content increases from the root zone (0 to 1.2 m) to the shallow vadose zone (< 3 m) or that the clay type is more reactive at greater depths. The deepest measuring σ_a for both 4mHcon and 4mPcon are equivalent to the 2mHcon data. This suggests that the deeper vadose zone (> 3 m) σ is equivalent to the shallow vadose zone and that soil properties are uniform. This is consistent with the known stratigraphy of the prior stream channels and clay alluvial plains as described by Stannard and Kelly (1968).

In order to better appreciate the DUALEM-421 σ_a data and confirm the inferences about σ above, the σ_a data is inverted using three different inversion programs. In the first instance *DUALEM-2d* (Santos et al., 2009) enabled a cross-sectional model of σ to be developed. This program is based on the cumulative function which provides a partial solution to the inverse problem, limited by the non-linearity of the σ_a in relation to the instrument response. The cross-section of σ generated across each transect is generally consistent with the known physiography across prior stream channels and clay alluvial plains of the lower Gwydir valley. Along transect 21.5, where soil particle size fractions and soil property data is available, the estimated σ values generally reflect the soil properties which

characterise these physiographic units. Specifically, small subsurface σ (0 to 200 mS/m) represent the smaller CEC, $EC_{1:5}$ and coarser textures (i.e. sandy loams) of the prior stream channels. Conversely, larger values of σ (> 400 mS/m) characterise the finer textured (i.e. medium to heavy clays) and slightly larger $EC_{1:5}$ of the root zone soil properties of the clay alluvial plain.

The second inversion program used is *DUALEM-2d-Full* (Santos, 2009). This algorithm accounts for the larger σ because it takes advantage of the full solution to the inverse problem and is not limited by the non-linearity problem. The σ models obtained portray the soil profile in a more realistic way when compared to the results from the *DUALEM-2d* inversion. Specifically, the small σ (< 150 mS/m) coincides with the small CEC, $EC_{1:5}$ and coarser textures of the prior stream channel. Conversely the layer of larger σ (> 400 mS/m) is evident in the deeper soil profile, within the shallow vadose zone, as opposed to the root zone and is a much thicker layer than how it appears in the σ models from the *DUALEM*-2d σ models. This is consistent with the soil particle size fraction information that was presented by Vervoort and Annen (2006) at a similar depth within the soil profile within the general area of the study site.

DUALEM-3d, a 1D spatially constrained inversion program produces a quasi-3D σ model. This inversion program delineates the main σ structure of the prior stream channel adjacent to the clay alluvial plain, but is also limited by the non-linearity of the cumulative function.

Despite the poor relationship established between the σ models obtained with the *DUALEM-2d* and *DUALEM-2d-Full* inversion algorithms and the clay content, $EC_{1:5}$ or CEC, the models did represent the overall change in soil properties and reflect the sediments associated with prior stream channels. The lack of statistical correlation (Pearson correlation coefficient values < 0.3) is attributed to a layer of small σ values within the upper 1 m of the

soil profile that may be affected by low moisture content in the topsoil at the time of the σ_a survey. Follow up research should be carried out in more favourable conditions (i.e. soon after irrigation or heavy rainfall) in order to determine the influence of surface soil moisture. Conversely, and in order to better represent and model the deeper vadose zone and characterise the connectivity between the prior stream channel and the palaeochannel a joint inversion of Geonics EM-34 (Geonics Inc., Mississauga, Ontario, Canada) data and the DUALEM-421 data presented herein can be considered for future work.

References

Aster, R.C., Borchers, B. and Thurber, C.H., 2005. Parameter estimation and inverse problems. Elsevier Academic Press, USA.

Auken, E., Pellerin, L., Christensen, N.B. and Sørensen, K., 2006. A survey of current trends in near-surface electrical and electromagnetic methods. Geophysics, 71(5): G249-G260.

Butler, B.E., Blackburn, G. and Hubble, G.D., 1983. "Soils: An Australian Viewpoint", In: Murray-Darling Plains. Division of Soils, CSIRO, pp. 231-240.

Callegary, J.B., Ferre, T.P.A. and Groom, R.W., 2007. Vertical spatial sensitivity and exploration depth of low-induction-number electromagnetic-induction instruments. Vadose Zone Journal, 6: 158-167.

Christensen, N.B., 1997. Electromagnetic subsurface imaging. A case for an adaptive born approximation. Surveys in Geophysics, 18: 477-510.

Dualem, 2008. DUALEM-421S user's manual. Dualem Inc., Milton, Ontario, Canada.

Gee, G.W. and Bauder, J.W., 1979. Particle size analysis by hydrometer: a simplified method for routine textural analysis and a sensitivity test of measurement parameters. Soil Science Society of America Journal, 43: 1004-1007.

Gomez-Trevino, E., Esparza, F.J. and Mendez-Delgado, S., 2002. New theoretical and practical aspects of electromagnetic soundings at low induction numbers. Geophysics, 67(5): 1441-1451.

Hendrickx, J.M.H., Borchers, B., Corwin, D.L., Lesch, S.M., Hilgendorf, A.C. and Schlue, J., 2002. Inversion of soil conductivity profiles from electromagnetic induction measurements: theory and experimental verification. Soil Science Society of America Journal, 66: 673-685.

Holmgren, G.G.S., Juve, R.L. and Geschwender, R.C., 1977. A mechanically controlled variable leaching device. Soil Science of America Journal, 41: 1207-1208.

Huckel, A., 2004. Estimating clay content and deep drainage at the field scale in the lower Gwydir RIver valley. Masters Thesis, University of Sydney, Sydney.

Kaufman, A.A. and Keller, G.V., 1983. Frequency and transient soundings. Methods in Geochemistry and Geophysics, No 16. Elsevier, New York.

Kothavala, Z., 1999. The duration and severity of drought over eastern Australia simulated by a coupled ocean-atmosphereGCM with a transient increase in CO2. Environmental Modelling and Software, 14(4): 243-252.

McNeill, J.D., 1980a. Electrical conductivity of Soils and Rocks. Technical Note TN5, Geonics Limited, Mississauga, Ontario Canada.

McNeill, J.D., 1980b. Electromagnetic Terrain Conductivity Measurement at Low Induction Numbers. Technical Note TN6, Geonics Limited, Mississauga, Ontario Canada.

Needham, P., 1991. The extent of degraded heavy clays and associated soils in north-western New South Wales, Department of Conservation and Land Management, Soil Conservation Service, Inverell Research Service Centre, New South Wales, Australia.

Peckham, 2000. The rainbow serpent http://www.didjshop.com/stories/rainbow.html, date accessed 01/05/09.

Pellerin, L. and Wannamaker, P.E., 2005. Multi-dimensional electromagnetic modeling and inversion with application to near-surface earth investigations. Computers and Electronics in Agriculture, 46(1-3): 71-102.

Rhoades, J.D., Raats, P.A.C. and Prather, R.J., 1976. Effects of liquid-phase electrical conductivity, water content, and surface conductivity on bulk soil electrical conductivity. Soil Science Society of America Journal, 40: 651-655.

Santos, F.A.M., 2004. 1-D laterally constrained inversion of EM34 profiling data. Journal of Applied Geophysics, 56: 123-134.

Santos, F.A.M., 2009. DUALEM-2D-Full, personal communication.

Santos, F.A.M., Triantafilis, J., Bruzgulis, K.E. and Roe, J.A.E., 2009. Inversion of DUALEM-421 profiling data using a 1-D laterally constrained algorithm. Vadose Zone Journal, submitted.

Stannard, M.E. and Kelly, I.D., 1968. Irrigation potential of the lower Gwydir valley, Water Conservation and Irrigation Commission, New South Wales, Australia.

Triantafilis, J., Huckel, A.I. and Odeh, I.O.A., 2001. Comparison of statistical prediction methods for estimating field-scale clay content using different combinations of ancillary variables. Soil Science, 166(6): 415-427.

Triantafilis, J., Huckel, A.I. and Odeh, I.O.A., 2003. Field-scale assessment of deep drainage risk. Irrigation Science, 21(4): 183-192.

Triantafilis, J., Lesch, S.M., Lau, K.L. and Buchanan, S.M., 2009a. Field level digital soil mapping of cation exchange capacity using electromagnetic induction and a hierarchical spatial regression model in the lower Namoi valley. Australian Journal of Soil Research, 47: accepted.

Triantafilis, J., Odeh, I.O.A., Jarman, A.L., Short, M.G. and Kokkoris, E., 2004. Estimating and mapping deep drainage risk at the district level in the lower Gwydir and Macquarie valleys, Australia. Australian Journal of Experimental Agriculture, 44(9): 893-912.

Triantafilis, J., Santos, F.A.M., Macaulay, S. and Buchanan, S.M., 2009b. 2-dimensional digital soil and regolith mapping using a laterally constrained inversion model and EM34 and EM38 signal data. Australian Journal of Soil Research - in review.

Tucker, B.M., 1974. Laboratory procedure for cation exchange measurements in soils. CSIRO Australia, Division of Soils. Technical Paper No. 23. CSIRO, Australia.

Vervoort, R.W. and Annen, Y.L., 2006. Palaeochannels in northern New South Wales: inversion of electromagnetic inuction data to infer hydrologically relevant stratigraphy. Australian Journal of Soil Research, 44: 35-45.

Wait, J.R., 1962. A note on the electromagnetic response of a stratified earth. Geophysics, 27(3): 382-385.

Yasserie, J., 2009. In the Womb of the Rainbow Serpent. http://www.artistwd.com/joyzine/australia/dreaming/womb.php, date accessed 01/05/09.

Appendix A – Apparent conductivity (σ_a) data

Transects 20.0 to 16.5

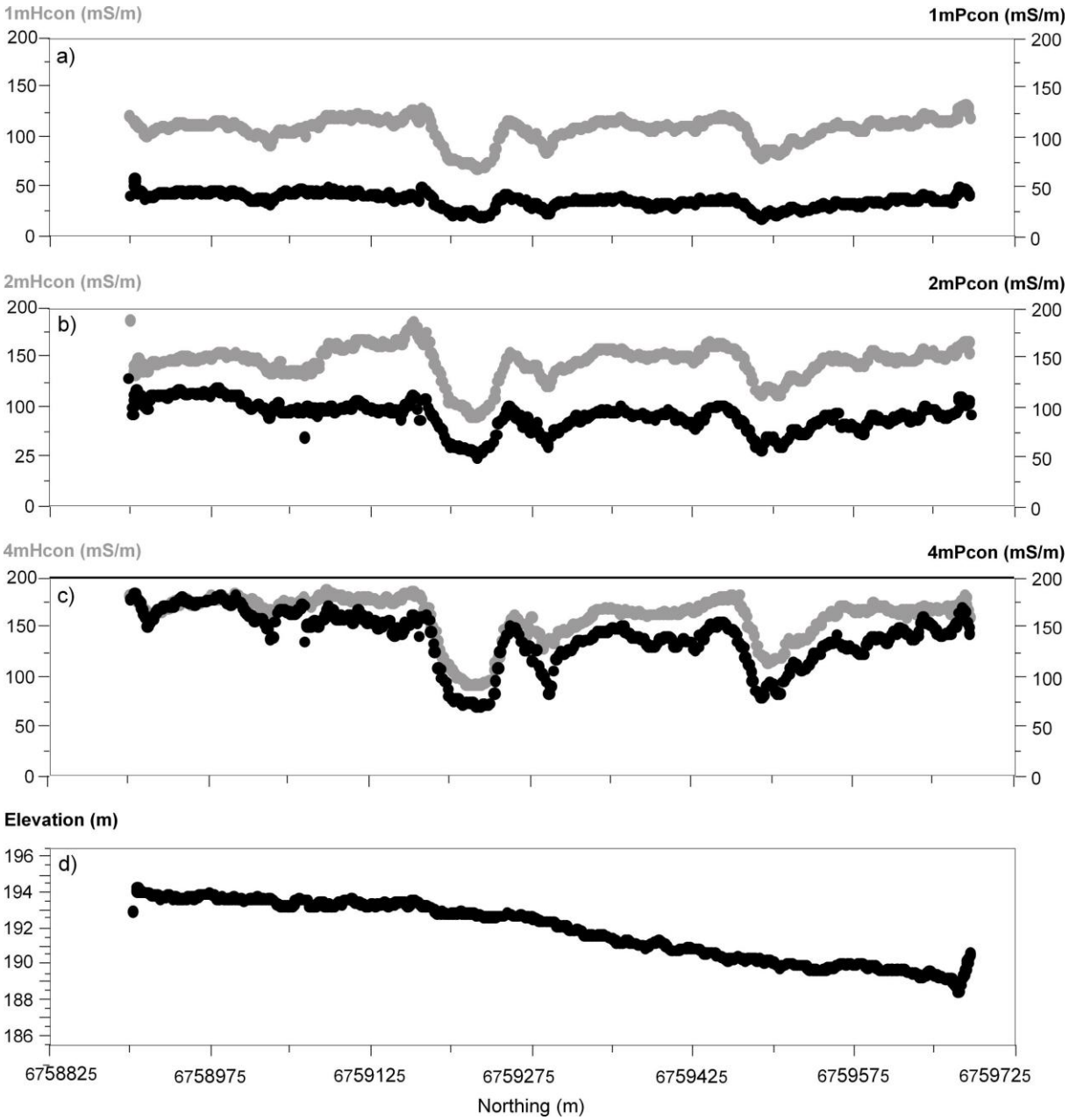

Fig. A1. Spatial distribution of apparent soil electrical conductivity (σ_a - mS/m) along transect 20.0 measured using a DUALEM-421 in horizontal coplanar (Hcon) and perpendicular (Pcon) modes of operation, and intercoil spacings of: a) 1m, b) 2m; and, c) 4m, and d) altitude (ASL - m).

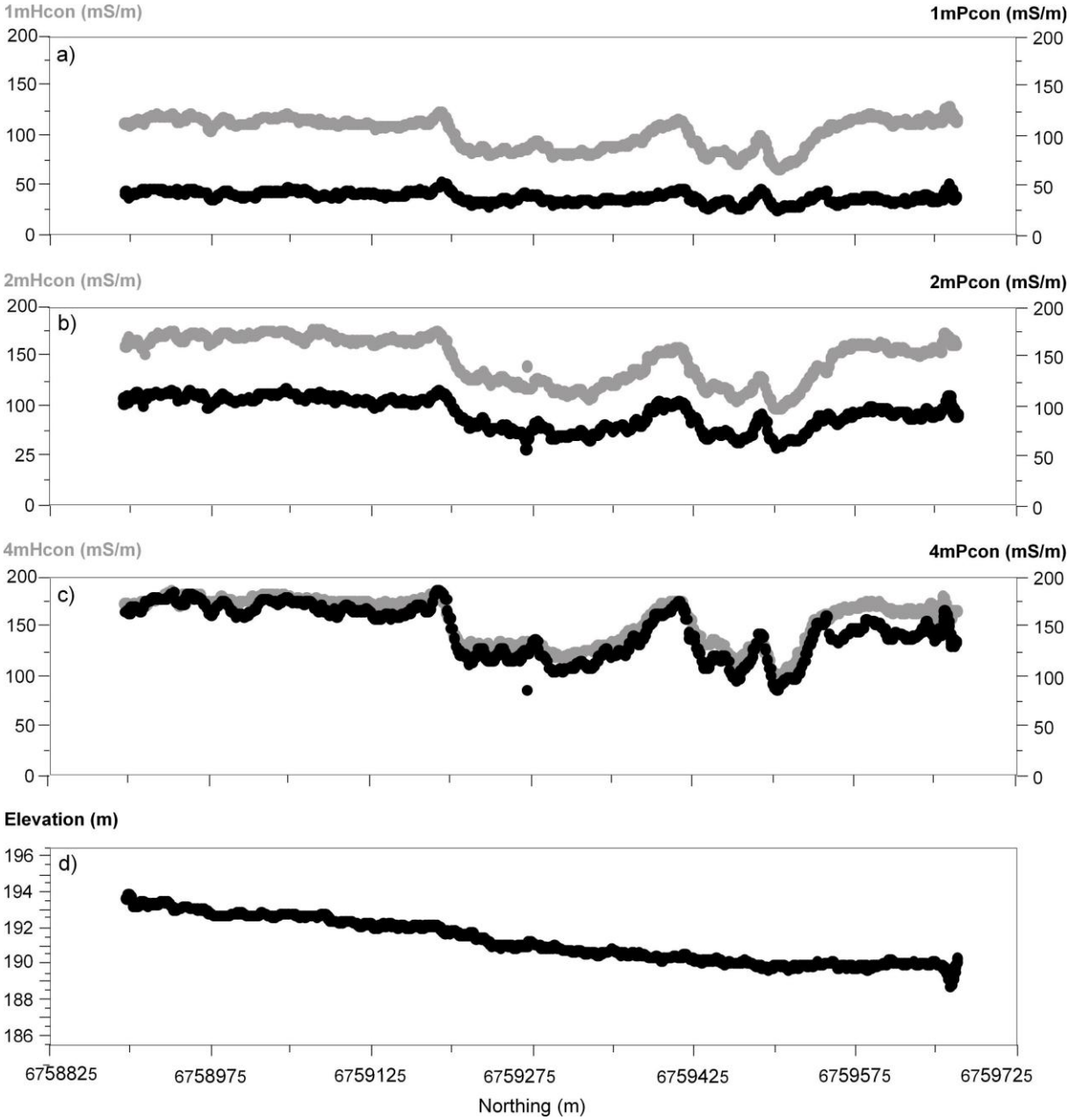

Fig. A2. Spatial distribution of apparent soil electrical conductivity (σ_a - mS/m) along transect 19.5 measured using a DUALEM-421 in horizontal coplanar (Hcon) and perpendicular (Pcon) modes of operation, and intercoil spacings of: a) 1m, b) 2m; and, c) 4m, and d) altitude (ASL - m).

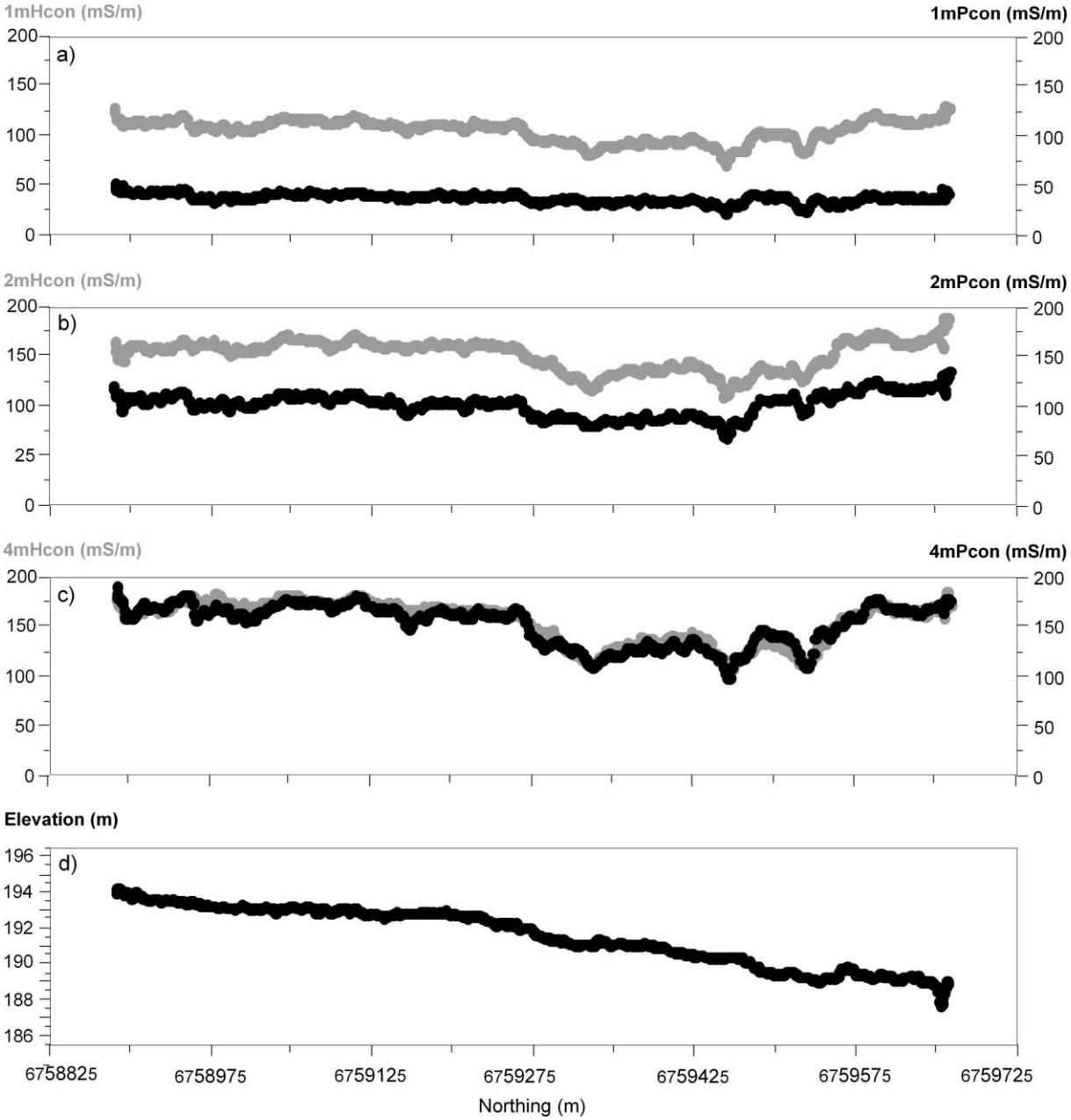

Fig. A3. Spatial distribution of apparent soil electrical conductivity (σ_a - mS/m) along transect 19.0 measured using a DUALEM-421 in horizontal coplanar (Hcon) and perpendicular (Pcon) modes of operation, and intercoil spacings of: a) 1m, b) 2m; and, c) 4m, and d) altitude (ASL - m).

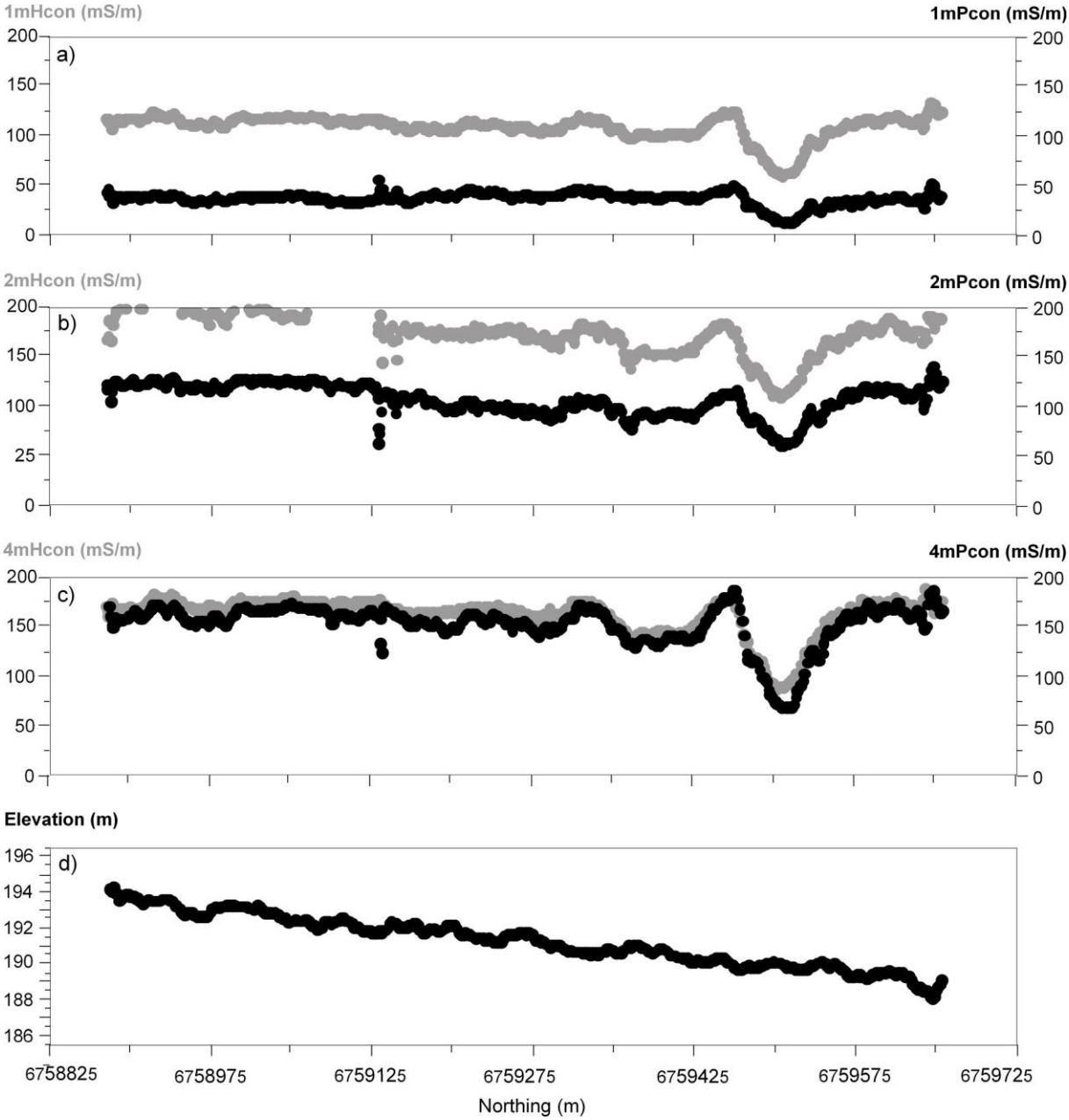

Fig. A4. Spatial distribution of apparent soil electrical conductivity (σ_a - mS/m) along transect 18.5 measured using a DUALEM-421 in horizontal coplanar (Hcon) and perpendicular (Pcon) modes of operation, and intercoil spacings of: a) 1m, b) 2m; and, c) 4m, and d) altitude (ASL - m).

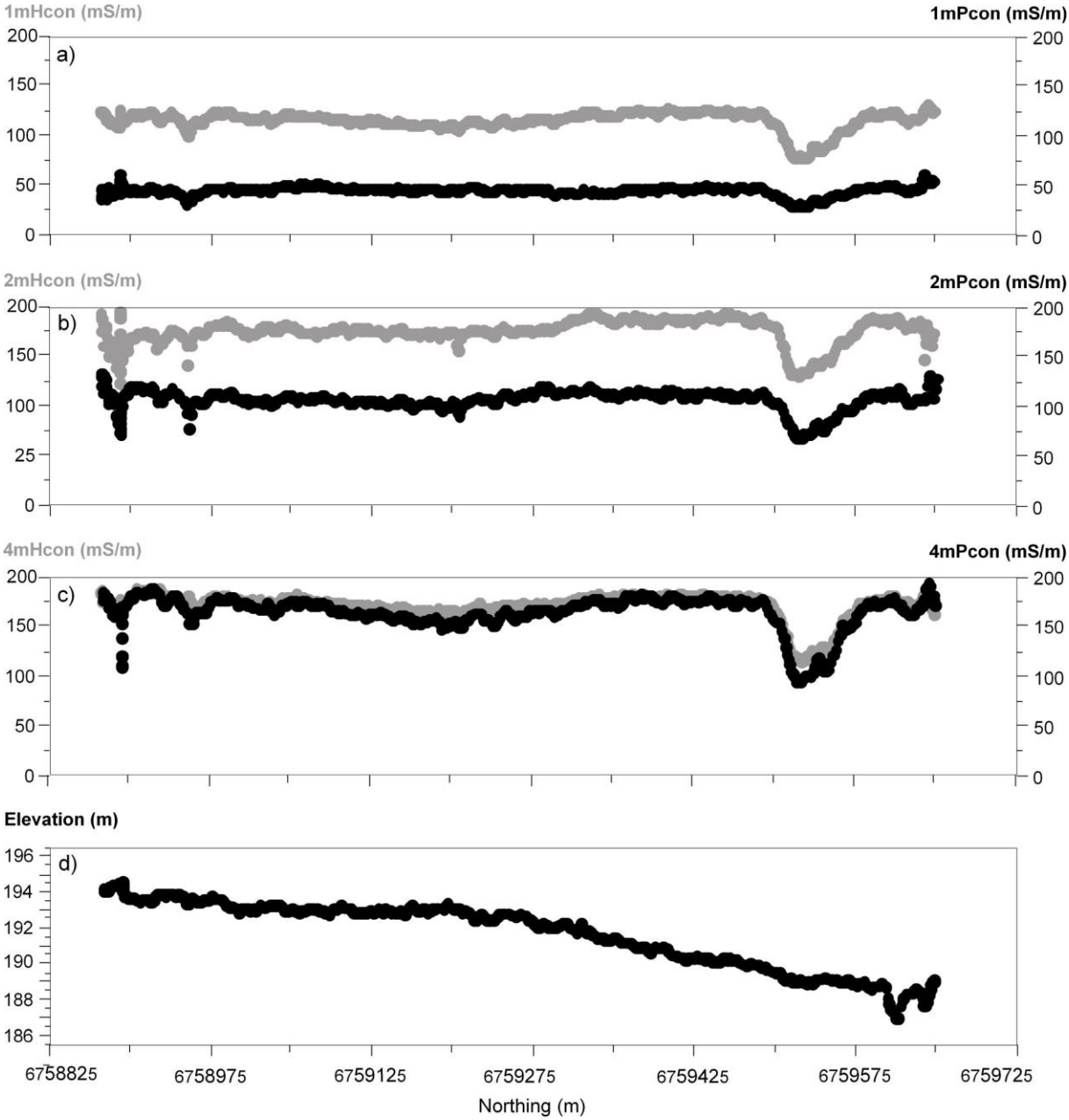

Fig. A5. Spatial distribution of apparent soil electrical conductivity (σ_a - mS/m) along transect 18.0 measured using a DUALEM-421 in horizontal coplanar (Hcon) and perpendicular (Pcon) modes of operation, and intercoil spacings of: a) 1m, b) 2m; and, c) 4m, and d) altitude (ASL - m).

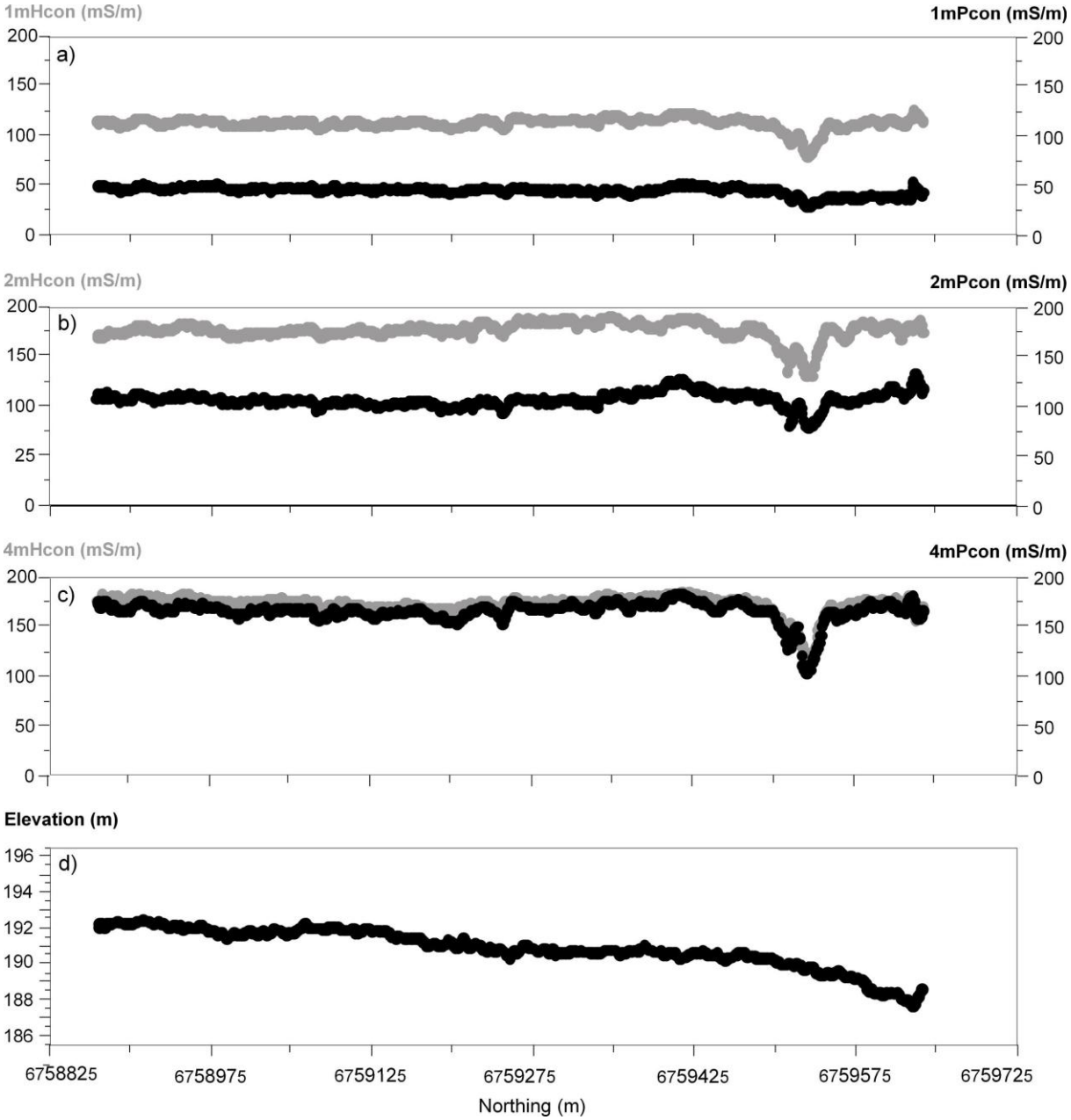

Fig. A6. Spatial distribution of apparent soil electrical conductivity (σ_a - mS/m) along transect 17.5 measured using a DUALEM-421 in horizontal coplanar (Hcon) and perpendicular (Pcon) modes of operation, and intercoil spacings of: a) 1m, b) 2m; and, c) 4m, and d) altitude (ASL - m).

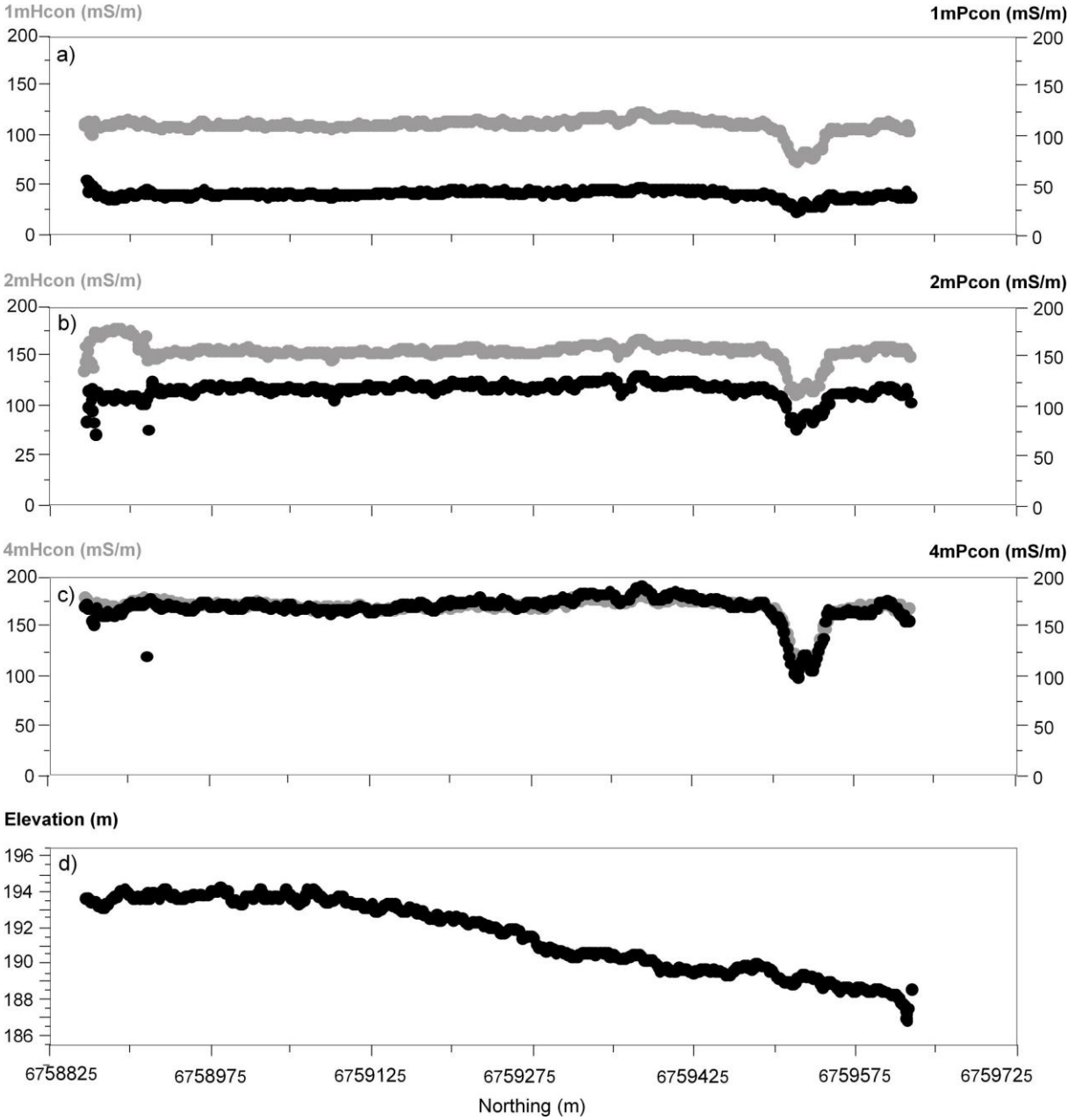

Fig. A7. Spatial distribution of apparent soil electrical conductivity (σ_a - mS/m) along transect 17.0 measured using a DUALEM-421 in horizontal coplanar (Hcon) and perpendicular (Pcon) modes of operation, and intercoil spacings of: a) 1m, b) 2m; and, c) 4m, and d) altitude (ASL - m).

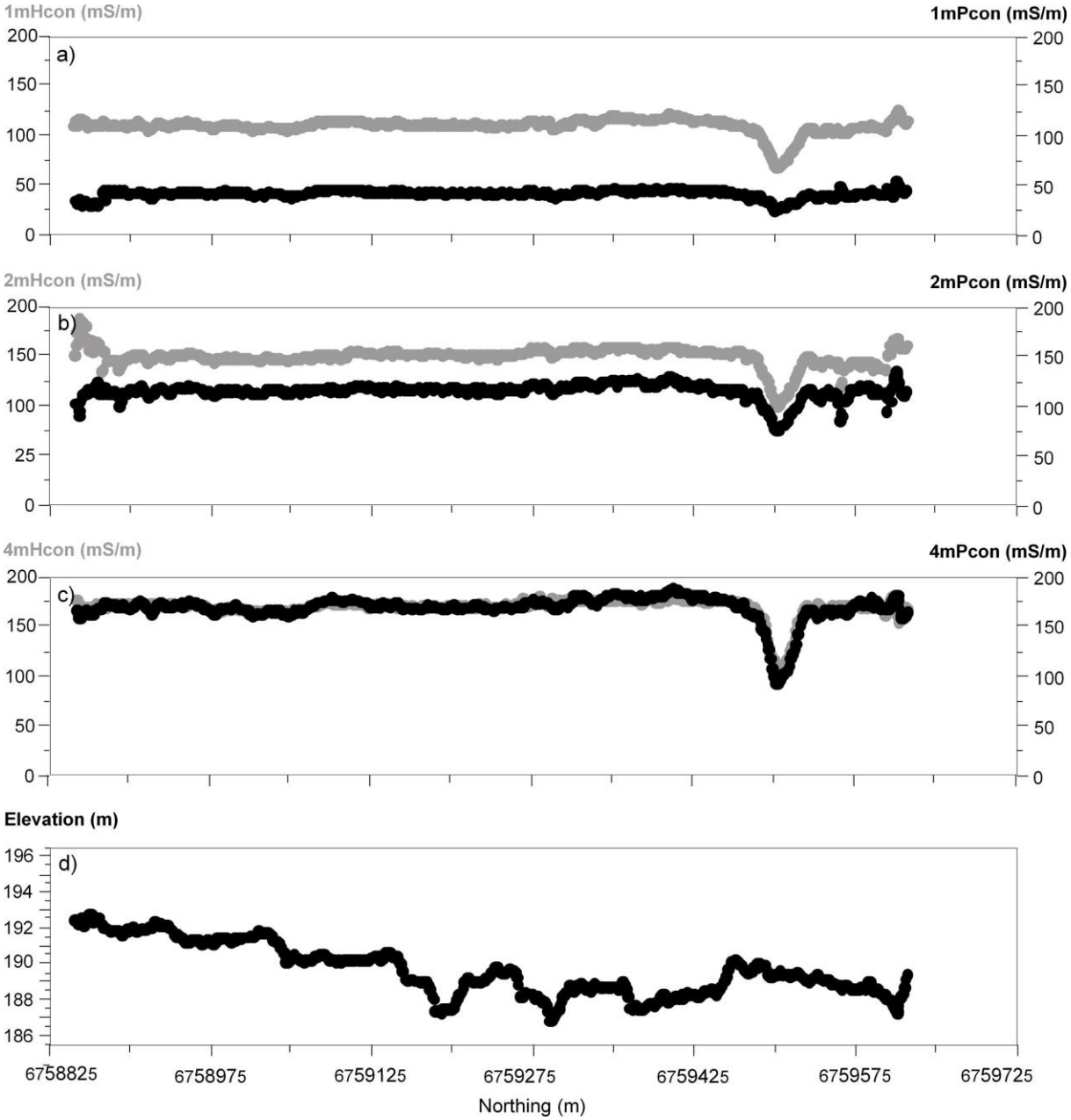

Fig. A8. Spatial distribution of apparent soil electrical conductivity (σ_a - mS/m) along transect 16.5 measured using a DUALEM-421 in horizontal coplanar (Hcon) and perpendicular (Pcon) modes of operation, and intercoil spacings of: a) 1m, b) 2m; and, c) 4m, and d) altitude (ASL - m).

Appendix B – Profile reconstruction using *DUALEM-2d*

Transects 20.0 to 16.5

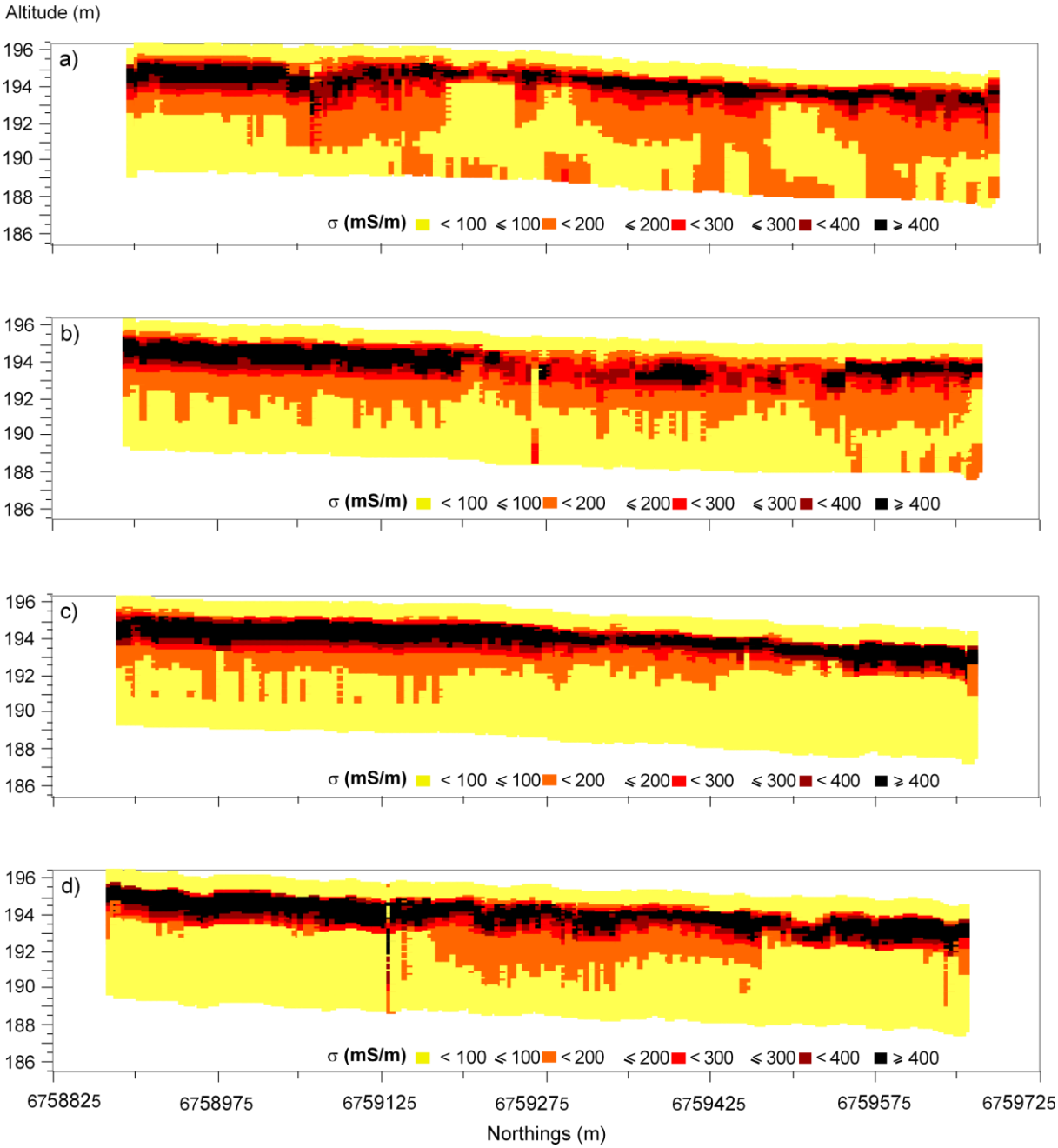

Fig. B1. 2-dimensional (2D) spatial distribution of soil electrical conductivity (σ - mS/m) obtained from *DUALEM-2d* and σ_a data along: a) transect 20.0, b) transect 19.5, c) transect 19.0, and d) transect 18.5.

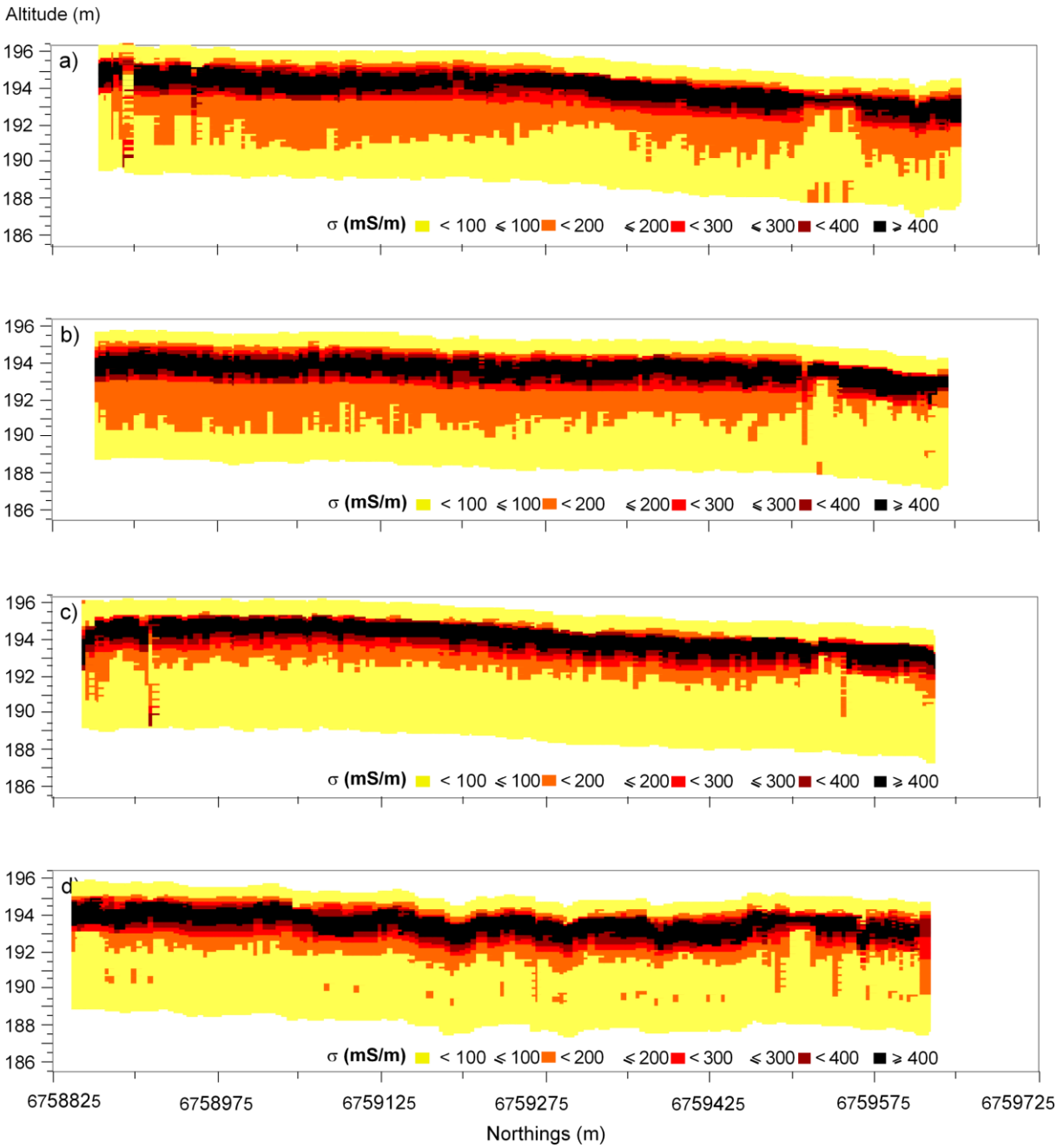

Fig. B2. 2-dimensional (2D) spatial distribution of soil electrical conductivity (σ - mS/m) obtained from *DUALEM-2d* and σ_a data along: a) transect 18.0, b) transect 17.5, c) transect 17.0, and d) transect 16.5.

Appendix C – Profile reconstruction using *DUALEM-2d-Full*

Transects 20.0 to 16.5

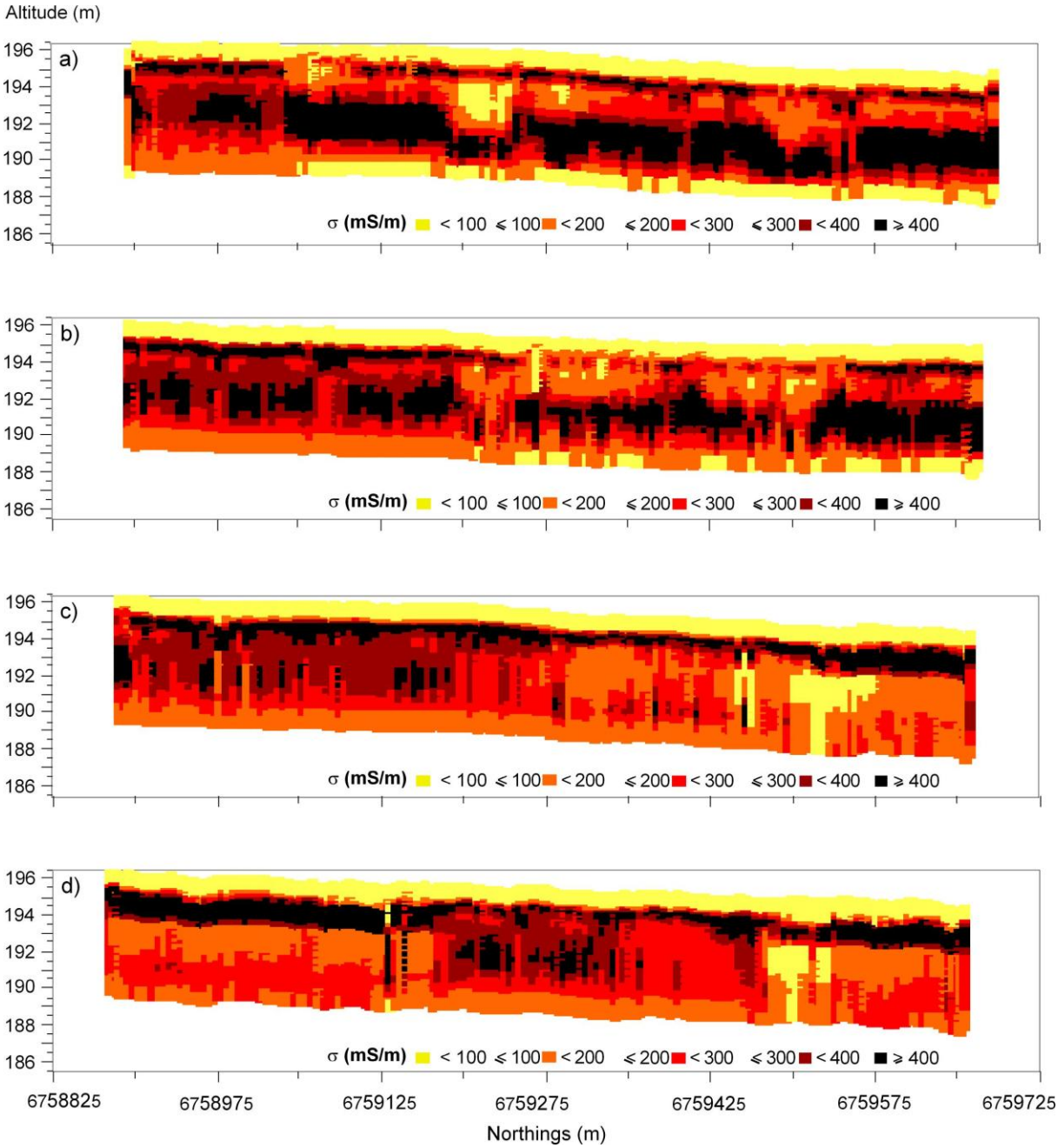

Fig. C1. 2-dimensional (2D) spatial distribution of soil electrical conductivity (σ - mS/m) obtained from *DUALEM-2d-Full* and σ_a data along: a) transect 20.0, b) transect 19.5, c) transect 19.0, and d) transect 18.5.

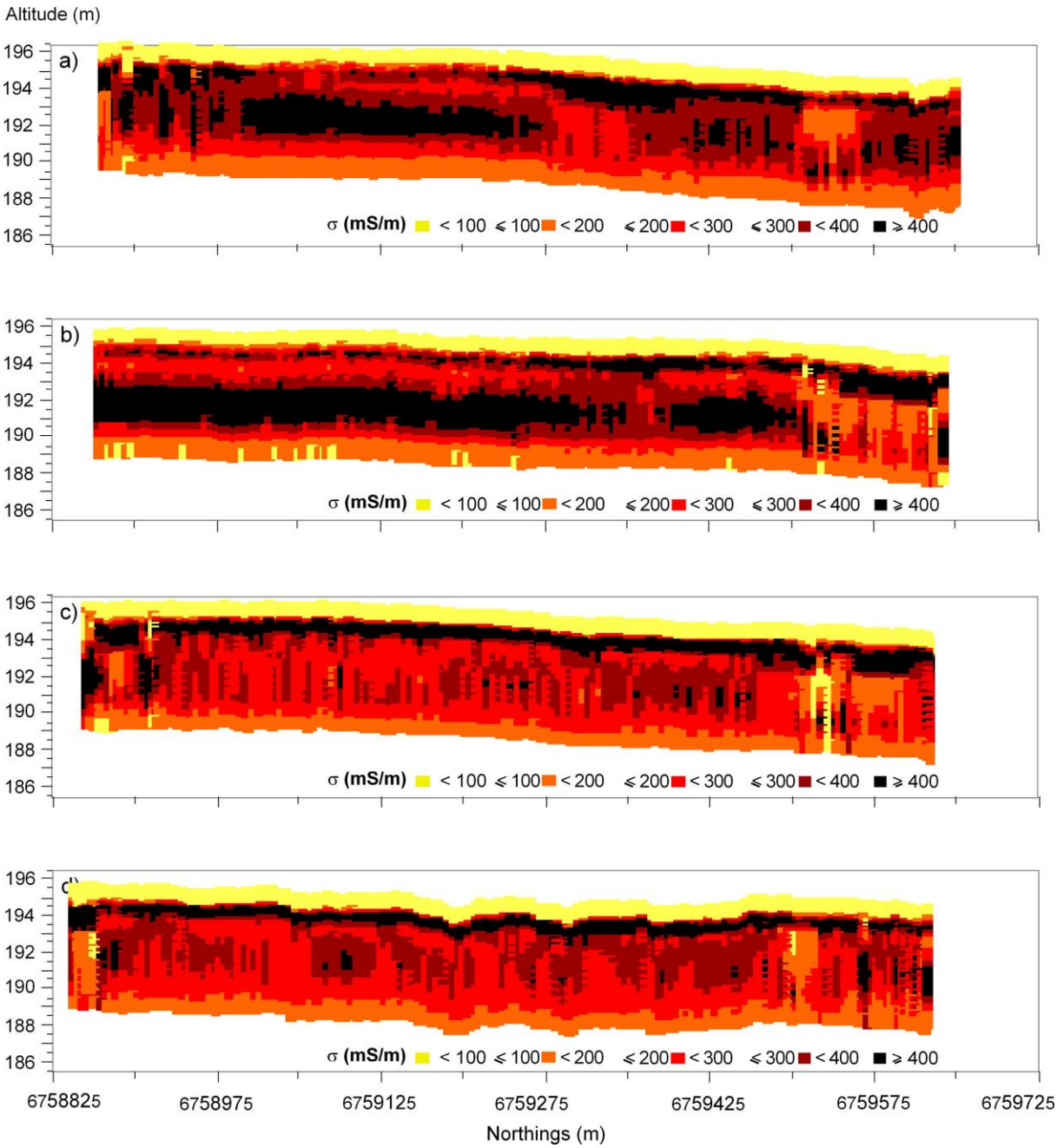

Fig. C2. 2-dimensional (2D) spatial distribution of soil electrical conductivity (σ - mS/m) obtained from DUALEM-2d-Full and σ_a data along: a) transect 18.0, b) transect 17.5, c) transect 17.0, and d) transect 16.5.